# A Comparative Study of Wavelets and Multiwavelets

by

Ellen Yanqing ZHENG

An M.Sc. Thesis

submitted to the School of Graduate Studies and Research
in partial fulfillment of the requirements for
the degree of Master of Science in Mathematics*

University of Ottawa
Ottawa, Ontario
Canada K1N 6N5

7 May 1996

*The M.Sc. Program is a joint program with
Carleton University, administered by the Ottawa-Carleton
Institute of Mathematics and Statistics

ISBN 0-612-20038-8

Canada

UNIVERSITÉ D'OTTAWA
UNIVERSITY OF OTTAWA

*To the memory of my father*

# Contents

# Abstract

In this thesis, some basic concepts and theorems are studied, leading to the cascade algorithm which is the most usual approximating method used in the construction of wavelets. By considering the symmetry property of scalar wavelets, Lawton's complex-valued scalar wavelets are studied and some recent results are implemented in the theory of complex-valued scalar wavelets. Another important part of this thesis is the study of multiwavelets. Some comparisons are made among real-valued scalar wavelets, complex-valued scalar wavelets and real-valued multiwavelets. A special contribution is the figures of different kinds of wavelets and some numerical results.

# Acknowledgements

I am deeply indebted to my thesis supervisor, Professor Rémi Vaillancourt, for his suggestions and very constructive criticism through the whole research period. I would also like to acknowledge his generous assistance with patient guidance during the preparation and writing of the thesis.

I gratefully acknowledge the Department of Mathematics and the University of Ottawa for providing me with financial support during my studies.

I am thankful to Professor Ryuichi Ashino from the Department of Mathematics, College of Industrial Technology, Amagasaki, Japan, for his advice and encouragements, as well as his comments on wavelet theory.

I would like to express my deep gratitude to Hai Yu for his unceasing encouragement and continuous support. I am also indebted to Dr. Abderrazek Karoui and Dr. Fadi Malek for their help.

Finally, I would like to give a very special thank to my family, and especially to my mother, Jinxia Li, who gave me her love and care.

# List of Tables

# List of Figures

# Chapter 1

# Introduction

Wavelets are mathematical functions that cut up data into different time and frequency components, and then studies each component with a resolution matched to its scale. They are a relatively recent development in applied mathematics. In the last twenty to thirty years, wavelets were developed independently in the fields of pure mathematics, engeneering and physics. Exchanges among these fields have led to many exciting applications.

The main branch of mathematics leading to wavelets began with Joseph Fourier with his Fourier synthesis. He observed that any "smooth" $2\pi$-periodic function $f(x)$ is the sum

$$a_0 + \sum_{k=1}^{\infty}(a_k \cos kx + b_k \sin kx)$$

of its Fourier series. Dirichlet's theorem states that if $f$ is continuous and piecewise differentiable, then the Fourier series converges pointwise. The coefficients $a_0$, $a_k$ and $b_k$ are calculated by the formulas

$$\begin{aligned} a_0 &= \frac{1}{2\pi}\int_0^{2\pi} f(x)\,dx, \\ a_k &= \frac{1}{\pi}\int_0^{2\pi} f(x)\cos kx\,dx, \\ b_k &= \frac{1}{\pi}\int_0^{2\pi} f(x)\sin kx\,dx. \end{aligned}$$

Problems arise from the difficulty of relating time and frequency properties of a function to those of its Fourier coefficients. An example that shows such difficulty was

given by J.-P. Kahane, Y. Katznelson and K. de Leeuw [19]. They showed that, to get a continuous function g(x) from an arbitrary square-summable function $f(x)$, it is sufficient to increase, or leave unchanged, the moduli of the Fourier coefficients of $f(x)$ and to adjust their phases judiciously. Thus, it is impossible to predict the properties (support length, regularity) of a function solely from the knowledge of the order of magnitude of its Fourier coefficients. Indeed, even if we know the Fourier coefficients explicitly, it is still difficult to predict these properties and many problems are still open.

At the begining of the 80's, many scientists used "wavelets" as an alternative to traditional Fourier Analysis. This alternative gave hopes for simpler numerical analysis and more robust synthesis of certain transitory phenomena.

The first mention of wavelets appeared in an appendix to the thesis of A. Haar in 1909 [17], where wavelet functions are defined as:

$$h_{jk}(x) = \begin{cases} 2^{-j/2} & 2^j(k-1) \leq x < 2^j(k-1/2), \\ -2^{-j/2} & 2^j(k-1/2) \leq x < 2^j k, \\ 0 & \text{otherwise.} \end{cases}$$

The Haar wavelets are compactly supported but their discontinuity somewhat limits their applications.

The theory of wavelets has been recently developed by A. Grossman and J. Morlet [16], Y. Meyer [32], S. Mallat [29], I. Daubechies [11] and others. A major achievement is due to the multiresolution analysis concept, introduced in 1986 by Y. Mayer and S. Mallat. Multiresolution analysis provides a natural framework for better understanding and designing wavelets. In 1987, I. Daubechies constructed for the first time a set of orthonormal and compactly supported wavelet basis functions which are perhaps the most elegant, and have become the cornerstone of wavelet applications today.

Wavelets are functions that satisfy certain mathematical requirements and are used in representing data or other functions. They are generated by translations and dilations of one basic function.

A one dimensional (1-D) orthonormal wavelet basis for $L^2(\mathbb{R})$ is a family of functions obtained by dilating and translating a "mother wavelet" $\psi \in L^2(\mathbb{R})$ :

$$\psi_{j,k}(x) = 2^{-j/2}\psi(2^{-j}x - k), \qquad x \in \mathbb{R},\ j,k \in \mathbb{Z},$$

satisfying

$$\int_{-\infty}^{\infty} \psi(t)\, dt = 0,$$

and

$$\int_{-\infty}^{\infty} \psi_{j,k}(x)\psi_{l,k}(x)\, dx = \delta_{j-l}.$$

So any $f$ in $L^2(\mathbb{R})$ can be written as

$$f(x) = \sum_{j\in\mathbb{Z}} \sum_{k\in\mathbb{Z}} < f, \psi_{j,k} > \psi_{j,k}(x)$$

where equality holds in the $L^2$-sense, and the coefficients are given by the scalar product

$$< f, \psi_{j,k} >= \int_{-\infty}^{\infty} f(x)\overline{\psi_{j,k}(x)}\, dx.$$

In wavelet analysis, the scale that one uses to look at data plays a special role. Wavelet algorithms process data at different scales or resolutions. In multiresolution analysis, scaling functions are defined by

$$\phi_{j,k}(x) = 2^{-j/2}\phi(2^{-j}x - k), \qquad x \in \mathbb{R},\ j,k \in \mathbb{Z},$$

with $\phi \in L^2(\mathbb{R})$. The functions $\phi_{0,n}(x) = \phi(x-n), n \in \mathbb{Z}$, constitute an orthonormal basis for a closed subspace $V_0$.

In contrast to single wavelet bases, multiwavelets correspond to many scaling functions. It is known that the oldest example of a function $\psi$ for which the $\psi_{j,k}$ defined by (1.1) constitute an orthonormal basis for $L^2(\mathbb{R})$ is the Haar function,

$$\psi(x) = \begin{cases} 1 & 0 \le x < \frac{1}{2}, \\ -1 & \frac{1}{2} \le x < 1, \\ 0 & \text{otherwise.} \end{cases}$$

Alpert generalized the Haar system to one-dimensional non-regular multiwavelets in $L^2(\mathbb{R})$ by producing an example of such multiwavelets. Using fractal interpolation, Geronimo, Hardin and Massopust [15] constructed a two-scaling function with short support and symmetry, and Donavan, Geronimo, Hardin and Massopust [14] constructed a corresponding two-wavelet also with short support and antisymmetry. Using matrix method in the time domain, Strang and Strela [36] constructed the D-G-H-M multiwavelet, and, in [37], they constructed a nonsymmetric pair. All these cases are in $L^2(\mathbb{R})$.

Because of the good localization in both the spatial and frequency domains, wavelets have found many applications in different fields, ranging from pure and applied mathematics, to physics and engineering.

In mathematics, wavelets are used to characterize some functional spaces, such as $L^p(\mathbb{R}^n)$ for $0 < p < \infty$, Hölder and Hardy spaces, etc. Applications of wavelet decompositions in numerical analysis, e.g., for solving partial differential equations, seem very promissing because of the "zooming" property which allows a very good representation of discontinuities, unlike the Fourier transform.

In physics, wavelets correspond to coherent states. In engineering, the exciting application of wavelets lies in signal analysis, such as sound synthesis and denoising images, etc..

It is well known that it is not possible for single wavelets with real-valued coefficients to have orthogonality, symmetry and compact support simultaneously, but this is possible for complex-valued wavelets and multiwavelets. Moreover, it is not very clear what is the difference between multiwavelets and complex-valued wavelets in their regularity, symmetry and support length. Due to the complication of construction of higher-dimensional wavelets, we are essentially concerned with the 1-D wavelets. In the following chapters, we shall study and make some comparison between complex-valued single wavelets and real-valued multiwavelets.

We should mention that this thesis is essentially based on published and submitted literature. Every chapter begins with a brief introduction in which we refer to the problem to be studied.

The work is organized as follows. In Chapter 2, we study and provide some design techniques for the construction of 1-D complex-valued orthonormal scalar wavelet bases with compact support and real-valued biorthogonal multiwavelet bases. Chapter 3 deals with complex-valued scalar wavelets. Chapter 4 describes multiwavelets. Chapter 5 contains numerical results and figures. Chapter 6 is the conclusion.

# Chapter 2

# Design of Wavelet Bases

The construction of Mayer's wavelets can be viewed as the first construction of smooth orthonormal wavelet bases. However, the advent of the concept of multiresolution analysis provides a natural framework for better designing wavelets. But to construct orthonormal wavelet bases with compact support, one may start from the filter or mask $m_0$ rather than from the scaling functions $\phi$ or vector spaces $V_j$ of a multiresolution analysis. In general, orthonormal wavelets cannot be written in closed form, but their graphs can be computed with arbitrarily high precision, via an algorithm which is called "cascade algorithm".

Except for the Haar bases, all the orthonormal wavelet bases with real coefficients cannot have symmetry and compact support simultaneously. Biorthogonal wavelet bases can overcome this shortcoming. In [3], it is shown that it is possible to construct symmetric biorthogonal wavelet bases with arbitrarily high preassigned regularity.

In this chapter, we study the necessary and sufficient condition of the existence of orthonormal wavelet bases and biorthogonal wavelet bases, and provide some techniques for designing them.

## 2.1 Multiresolution analysis

Wavelets have been introduced by A. Grossman and J. Morlet [16] as functions whose translations and dilations can be used for expansions in $L^2(\mathbb{R})$. The construction of a smooth wavelet basis is generally related to a multiresolution analysis.

**Definition 2.1** *A multiresolution analysis, MRA, consists of a decreasing sequence of closed linear subspaces of* $L^2(\mathbb{R})$ *satisfying*

$$\ldots V_2 \subset V_1 \subset V_0 \subset V_{-1} \subset V_{-2} \subset \ldots \tag{2.1}$$

*with*

$$\overline{\bigcup_{j\in\mathbf{Z}} V_j} = L^2(\mathbb{R}), \tag{2.2}$$

$$\bigcap_{j\in\mathbf{Z}} V_j = \{0\} \tag{2.3}$$

*and*

$$f \in V_j \Leftrightarrow f(2^j\cdot) \in V_0, \qquad \forall\, j \in \mathbb{Z}, \tag{2.4}$$

$$f \in V_0 \Rightarrow f(\cdot - k) \in V_0, \qquad \forall\, k \in \mathbb{Z}, \tag{2.5}$$

$$\exists\, \phi \in V_0 \text{ such that } \phi_{0,n}(x) = \phi(x-n) \text{ is an orthonormal basis of } V_0. \tag{2.6}$$

Together, (2.4), (2.5) and (2.6) imply that, for any $j \in \mathbb{Z}$,

$$\{\phi_{j,k}(x) = 2^{-j/2}\phi(2^{-j}x - k);\ k \in \mathbb{Z}\}$$

is an orthonormal basis for $V_j$.

The basic tenet of a multiresolution analysis is that there always exists an orthonormal wavelet basis $\{\psi_{j,k}\}_{j,k\in\mathbf{Z}}$ of $L^2(\mathbb{R})$ whenever a set of closed subspaces satisfies (2.1)– (2.6), where $\psi_{j,k}(x) = 2^{-j/2}\psi(2^{-j}x - k)$.

For each $j \in \mathbb{Z}$, define $W_j$ to be the orthogonal complement of $V_j$ in $V_{j-1}$, i.e., $V_{j-1} = V_j \bigoplus W_j$; then $W_j \perp W_{j'}$, if $j \neq j'$. We now have

$$L^2(\mathbb{R}) = \bigoplus_{j\in\mathbf{Z}} W_j$$

and

$$f \in W_j \Leftrightarrow f(2^j\cdot) \in W_0. \tag{2.7}$$

Our objective is thus to find $\psi \in W_0$ such that $\{\psi(\cdot - k)\}_{k\in\mathbf{Z}}$ constitute an orthonormal basis for $W_0$.

Since $V_0 \subset V_{-1}$, there exists a sequence of complex numbers $\{h_n\}_{n\in\mathbf{Z}}$ such that

$$\phi(x) = \sum_n h_n \phi_{-1,n}(x) = \sqrt{2} \sum_n h_n \phi(2x - n) \tag{2.8}$$

with

$$h_n =< \phi, \phi_{-1,n} >= \sqrt{2} \int_{-\infty}^{+\infty} \phi(x)\overline{\phi(2x - n)}\, dx. \tag{2.9}$$

The Fourier transform of (2.8) is

$$\widehat{\phi}(\xi) = \frac{1}{\sqrt{2}} \sum_n h_n\, e^{-in\xi/2} \widehat{\phi}(\xi/2) := m_0(\xi/2)\widehat{\phi}(\xi/2). \tag{2.10}$$

From this definition of $m_0(\xi)$, we can see that $m_0$ is a $2\pi$-periodic function in $L^2([0, 2\pi])$.

A necessary condition to obtain a continuous scaling function $\phi \in L^2(\mathbb{R})$ is

$$|m_0(\xi)|^2 + |m_0(\xi + \pi)|^2 = 1 \qquad \text{a.e.} \tag{2.11}$$

and

$$m_0(0) = 1. \tag{2.12}$$

It is proved in [11], pp. 131–135, that if we define a basic wavelet function $\psi$ as

$$\psi = \sum_n (-1)^n \overline{h_{-n+1}}\, \psi_{-1,n},$$

i.e.,

$$\psi(x) = \sqrt{2} \sum_n (-1)^n\, \overline{h_{-n+1}}\, \psi(2x - n), \tag{2.13}$$

then $\{\psi_{0,n}\}_{n\in\mathbf{Z}}$ constitute an orthonormal basis of $W_0$. Thus, we see from formula (2.7) that for any $j \in \mathbb{Z}$, $\{\psi_{j,n}\}_{n\in\mathbf{Z}}$ is an orthonormal basis for $W_j$. Consequently, the collection of $\{\psi_{j,n}\}_{j,n\in\mathbf{Z}}$ constitute an orthonormal basis for $L^2(\mathbb{R})$.

The functions $\phi_{j,k}(x)$, $\psi_{j,k}(x)$ and $m_0(\xi)$ have special names as in the following definition.

**Definition 2.2** *For a given multiresolution analysis, MRA,*

1. *the functions* $\phi_{j,k}$, $j,k \in \mathbb{Z}$, *are called scaling functions generated from the (father) scaling function* $\phi(x)$

2. *the functions* $\psi_{j,k}$, $j,k \in \mathbb{Z}$, *are called wavelets generated from the mother wavelet* $\psi(x)$.

3. $m_0(\xi) = \frac{1}{\sqrt{2}} \sum_{n\in\mathbb{Z}} h_n e^{-in\xi}$ *is the frequency response of the filter associated with the multiresolution analysis MRA.*

**Remark 2.1** *In the previous discussion, we proved that we can derive an orthonormal wavelet basis from any multiresolution analysis. However, it is not true that any wavelet is related to a multiresolution analysis. The following counterexample is due to Y. Meyer [32]:*

$$\widehat{\psi}(w) = \begin{cases} 1 & \text{if } \frac{4\pi}{7} \le |w| \le \pi \text{ or } 4\pi \le |w| \le 4\pi + \frac{4\pi}{7}, \\ 0 & \text{otherwise.} \end{cases}$$

*The translates and dilates*

$$2^{-j/2}\psi(2^{-j}x - k) \qquad k, j \in \mathbb{Z}$$

*of* $\psi$ *constitute an orthonormal basis of* $L^2(\mathbb{R})$. *Suppose the vector space* $V_J$ *is generated by*

$$V_J = span\{\psi_{j,k} = 2^{-j/2}\psi(2^{-j}x - k);\ k \in \mathbb{Z},\ -\infty < j < J\},$$

*We can verify that the sequence of vector spaces* $(V_J)_{J\in\mathbb{Z}}$ *does not satisfy condition* (2.4).

Similar to the orthonormal wavelet case, the theory of biorthogonal wavelets is also based on the idea of a biorthogonal multiresolution analysis, which is a double multiresolution analysis. The difference is that biorthogonal wavelets have biorthogonal scaling functions.

**Definition 2.3** *A biorthogonal multiresolution analysis, BMRA, consists of two single multiresolution analysis ladders:*

$$\{0\} \to \ldots V_2 \subset V_1 \subset V_0 \subset V_{-1} \subset V_{-2} \subset \ldots \to L^2(\mathbb{R}), \tag{2.14}$$

$$\{0\} \to \ldots \widetilde{V}_2 \subset \widetilde{V}_1 \subset \widetilde{V}_0 \subset \widetilde{V}_{-1} \subset \widetilde{V}_{-2} \subset \ldots \to L^2(\mathbb{R}), \tag{2.15}$$

*with*

$$V_0 = \overline{span\,\{\phi_{0,k};\ k \in \mathbb{Z}\}}, \qquad \widetilde{V}_0 = \overline{span\,\{\widetilde{\phi}_{0,k};\ k \in \mathbb{Z}\}}, \tag{2.16}$$

*where $\phi_{0,k}$ and $\widetilde{\phi}_{0,k}$, for $k \in \mathbb{Z}$, are so-called scaling functions.*

*In addition, the two multiresolutions are related to each other by the biorthogonal conditions:*

$$V_j \perp \widetilde{W}_j, \qquad \widetilde{V}_j \perp W_j, \tag{2.17}$$

*where $W_j$ and $\widetilde{W}_j$ are the (non-orthonormal) complements of $V_j$ and $\widetilde{V}_j$ in $V_{j-1}$ and $\widetilde{V}_{j-1}$, respectively.*

Like the situation in the orthonormal wavelet case, for fixed $j \in \mathbb{Z}$,

$$W_j = \overline{\text{span}\,\{\psi_{j,k}\}}_{k\in\mathbb{Z}} \qquad \widetilde{W}_j = \overline{\text{span}\,\{\widetilde{\psi}_{j,k}\}}_{k\in\mathbb{Z}}.$$

The biorthogonal wavelets with dilation factor 2, $\psi_{j,k}(x)$ and $\widetilde{\psi}_{j,k}(x)$, derived from two mother wavelets, $\psi(x)$ and $\widetilde{\psi}(x)$ ,respectively, are a pair of families of dual wavelets defined as

$$\psi_{j,k}(x) = 2^{-j/2}\psi(2^{-j}x - k), \qquad \widetilde{\psi}_{j,k}(x) = 2^{-j/2}\widetilde{\psi}(2^{-j}x - k). \tag{2.18}$$

Therefore, any $f$ in $L^2(\mathbb{R})$ can be expanded into the series

$$\begin{aligned} f &= \sum_{j,k} < f, \psi_{j,k} > \widetilde{\psi}_{j,k} \\ &= \sum_{j,k} < f, \widetilde{\psi}_{j,k} > \psi_{j,k}. \end{aligned} \tag{2.19}$$

Once we have the basic idea of construction of wavelet and biorthogonal wavelet bases, the stimulating questions then arise: what is the necessary and sufficient condition for the existence of orthonormal wavelet and biorthogonal wavelets bases, and how to construct them? Some answers, given in [11] and [3], are briefly summarized in the following sections.

## 2.2 Compactly supported orthonormal wavelet bases

From the basic idea of multiresolution analysis for constructing orthonormal wavelet bases, we can see that the easiest way to ensure compact support for the wavelet $\psi$ is to choose a compactly supported scaling function $\phi$.

By (2.9), for compactly supported $\phi$, only finitely many $h_n$ are nonzero, and the $2\pi$-periodic function $m_0$,

$$m_0(\xi) = \frac{1}{\sqrt{2}} \sum_n h_n \, e^{-in\xi}, \tag{2.20}$$

is a trigonometric polynomial. The orthonormality of $\phi_{0,n}$ gives

$$|m_0(\xi)|^2 + |m_0(\xi + \pi)|^2 = 1. \tag{2.21}$$

In constructing wavelet bases, we are also interested in making $\phi$ and $\psi$ reasonably regular. To do so, we have the following theorem.

**Theorem 2.1** *Assume that $\psi_{j,k}$ constitute an orthonormal basis of wavelets associated with a multiresolution analysis. If*

$$|\phi(x)| \le C(1 + |x|)^{-m-1-\varepsilon}, \qquad |\psi(x)| \le C(1 + |x|)^{-m-1-\varepsilon},$$

*and $\psi \in C^m$ with $\psi^{(l)}$ bounded for $l \le m$, then $m_0$, defined by* (2.9) *and* (2.10), *factorizes as*

$$m_0(\xi) = \left(\frac{1 + e^{i\xi}}{2}\right)^{m+1} \mathcal{L}(\xi), \tag{2.22}$$

*where $\mathcal{L}$ is $2\pi$-periodic and $\mathcal{L} \in C^m$.*

PROOF. The proof proceeds by induction on $l$. It uses a Taylor expansion and the facts that the dyadic rationals $2^{-j}k$, $(j, k \in \mathbb{Z})$ are dense in $\mathbb{R}$ and the Fourier transform of $x^l f(x)$ is $i^l \widehat{\psi}^{(l)}(\xi)$. For the detail, see [11], pp. 155–156. □

The existence of $m_0$ of the form in (2.22) is discussed in the following two propositions.

**Proposition 2.1** *A trigonometric polynomial $m_0$ of the form*

$$m_0(\xi) = \left(\frac{1+e^{-i\xi}}{2}\right)^N \mathcal{L}(\xi) \tag{2.23}$$

*satisfies* (2.21) *if and only if* $L(\xi) = |\mathcal{L}(\xi)|^2$ *can be written as*

$$L(\xi) = P(\sin^2(\xi/2)),$$

*with*

$$P(y) = P_N(y) + y^N R\left(\frac{1}{2} - y\right), \tag{2.24}$$

*where*

$$P_N(y) = \sum_{k=0}^{N-1} \binom{N-1+k}{k} y^k \tag{2.25}$$

*and $R$ is an odd polynomial, chosen such that $P(y) \geq 0$ for $y \in [0,1]$.*

PROOF. If we let

$$\begin{aligned} M_0(\xi) &= |m_0(\xi)|^2 \\ &= (\cos^2 \xi/2)^N L(\xi) \\ &= (\cos^2 \xi/2)^N P(\sin^2 \xi/2), \end{aligned}$$

the proof of the proposition follows from Bezout's theorem applied to

$$(1-y)^N P(y) + y^N P(1-y) = 1.$$

For the detail, see [11], pp. 168–171. □

The following proposition due to Riesz is used in the spectral factorization of $L(\xi)$.

**Proposition 2.2 (Riesz Lemma)** *Let $A$ be a positive trigonometric polynomial invariant under the substitution $\xi \to -\xi$; hence $A$ is necessarily of the form*

$$A(\xi) = \sum_{m=0}^{M} a_m \cos(m\xi), \qquad \text{with } a_m \in \mathbb{R}.$$

*Then there exist a trigonometric polynomial $B$ of order $M$, i.e.,*

$$B(\xi) = \sum_{m=0}^{M} b_m e^{im\xi}, \qquad \text{with } b_m \in \mathbb{R},$$

*such that $|B(\xi)|^2 = A(\xi)$.*

PROOF. The proof given in [11], pp. 172–173, is constructive and can be found below in Section 2.4. □

Although the above propositions ensure the existence of $m_0$, not every such $m_0$ leads to an orthonormal wavelet basis. We need additional conditions.

For this purpose, we define some terms to be used later.

**Definition 2.4** *A family of functions $\{\phi_j\}_{j\in J}$ in a Hilbert space $\mathcal{H}$ is called a frame if there exist constants $A > 0$, $B < \infty$ such that, for all $f$ in $\mathcal{H}$,*

$$A\|f\|^2 \leq \sum_{j\in J} |< f, \phi_j >|^2 \leq B\|f\|^2.$$

*We call $A$ and $B$ the frame bounds. If the frame bounds are equal, $A = B$, then we call the frame a tight frame.*

**Definition 2.5** *The sequence $\{\mu_n\}_{n\in\mathbb{N}}$ is a Riesz basis in a Hilbert space $\mathcal{H}$ if and only if*

1. *The closure of the finite linear span of the $\mu_n$ is $\mathcal{H}$, and*
2. *$\exists\, A > 0, B < \infty$ such that*

$$A\sum_n |C_N|^2 \leq \|\sum_n C_n\mu_n\|^2 \leq B\sum_n |C_n|^2$$

*for all $C = \{C_n\}_{n\in\mathbb{N}} \in l^2(\mathbb{N})$.*

The following proposition follows from the general theory.

**Proposition 2.3** *The sequence $\{\mu_n\}_{n\in\mathbb{N}}$ is a Riesz basis if and only if*

1. *The $\mu_n$ are independent, i.e., no $\mu_{n_0}$ lies within the closure of the finite linear span of the other $\mu_n$, and*
2. *$\exists\, A > 0$, $B > \infty$ such that*

$$A\,\|f\|^2 \leq \sum_n |< f, \mu_n >|^2 \leq B\|f\|^2, \quad \text{for all} \quad f \in \mathcal{H}.$$

In [3]), it is mentioned that characterisation 1 is used more frequently.

**Theorem 2.2** *Suppose $m_0$ is a trigonometric polynomial such that $|m_0(\xi)|^2+|m_0(\xi+\pi)|^2 = 1$ and $m_0(0) = 1$. Define $\phi$ and $\psi$ by*

$$\widehat{\phi}(\xi) = (2\pi)^{-1/2}\prod_{j=1}^{\infty} m_0(2^{-j}\xi),$$
$$\widehat{\psi}(\xi) = e^{-i\xi/2}\overline{m_0(\xi/2+\pi)}\widehat{\phi}(\xi/2).$$

*Then $\phi$ and $\psi$ are compactly supported $L^2$-functions, satisfying*

$$\phi(x) = \sqrt{2}\sum_n h_n\phi(2x-n),$$

$$\psi(x) = \sqrt{2}\sum_n (-1)^n h_{-n+1}\phi(2x-n)$$

*where $h_n$ is determined by $m_0$ via $m_0(\xi) = \frac{1}{\sqrt{2}}\sum_n h_n e^{-in\xi}$. Moreover, the family of functions $\{\psi_{j,k}(x) = 2^{-j/2}\psi(2^{-j}x-k);\ j,k\in\mathbb{Z}\}$ constitute a tight frame for $L^2(\mathbb{R})$ with frame constant 1. This tight frame is an orthonormal basis if and only if $m_0$ satisfies one of the following equivalent conditions:*

1. *There exists a compact set $K$, congruent to $[-\pi,\pi]$ modulo $2\pi$, containing a neighborhood of 0, such that*

$$\inf_{k>0}\inf_{\xi\in K}|m_0(2^{-k}\xi)| > 0.$$

2. *There exists no nontrivial cycle $\{\xi_1,\xi_2,\ldots,\xi_n\}$ in $[0,2\pi)$, invariant under $\tau:\ \xi\to 2\xi$ modulo $2\pi$, such that $m_0(\xi_j+\pi) = 0$ for all $j = 1,\ldots,n$.*

3. *The eigenvalue 1 of the $[2(N_2-N_1)-1]\times[2(N_2-N_1)-1]$ matrix $A$ defined by*

$$A_{lk} = \sum_{n=N_1}^{N_2} h_n\overline{h_{k-2l+n}}, \qquad -(N_2-N_1)+1\le l,k\le(N_2-N_1)+1,$$

*is simple (here we have assumed that $h_n = 0$ for $n < N_1$ and $n > N_2$).*

PROOF. The proof, which is long, can be found in [11], pp. 174–194. This theorem summarizes deep results of Mallat [29], Cohen [2], Lawton [23], [24], Cohen, Daubechies and Fauveau [3]. In the course of the proof, use is made of a result of

Deslauriers and Dubuc [13] on the compactness of the Fourier transform of distribution, stated as Lemma 2.1 below. □

This theorem tells us that we "almost always" have a corresponding orthonormal wavelet basis provided $m_0(0) = 1$.

**Remark 2.2** **(i)** *A compact set $K$ is called congruent to $[-\pi, \pi]$ modulo $2\pi$ if*

1. $|K| = 2\pi$,
2. *For all $\xi$ in $[-\pi, \pi]$, there exists $l \in \mathbb{Z}$ so that $\xi + 2l\pi \in K$.*

**(ii)** *A special case for condition 2 is $\xi_1 = -\frac{\pi}{3}$, $\xi_2 = \frac{\pi}{3}$. Cohen [2] summarized this specific equivalent condition as follows: Under the conditions in Theorem 2.2, if $m_0$ has no zeros in $[-\pi/3, \pi/3]$, then $\phi_{0,n}$ are orthonormal. The conclusion is optimal because it is not possible to find $\alpha < \frac{1}{3}$ such that the absence of zeros of $m_0$ in $[-\alpha\pi, \alpha\pi]$ guarantees orthonormality of $\phi_{0,n}$.*

*For instance,*

$$m_0(\xi) = \frac{1}{2}(1 + e^{-3i\xi}) = e^{-3i\xi/2} \cos \frac{3\xi}{2}.$$

*This $m_0$ satisfies*

$$|m_0(\xi)|^2 + |m_0(\xi + \pi)|^2 = 1 \quad \textit{and} \quad m_0(0) = 1.$$

*Substituting $m_0(\xi)$ into*

$$\widehat{\phi}(\xi) = (2\pi)^{-1/2} \prod_{j=1}^{\infty} m_0(2^{-j}\xi)$$

*leads to*

$$\begin{aligned} \widehat{\phi}(\xi) &= (2\pi)^{-1/2} \prod_{j=1}^{\infty} e^{-3i2^{-j}\xi/2} \cos\left(\frac{3}{2} 2^{-j}\xi\right) \\ &= (2\pi)^{-1/2} e^{-3i\xi/2} \prod_{j=1}^{\infty} \cos\left(\frac{3}{2} 2^{-j}\xi\right) \\ &= (2\pi)^{-1/2} e^{-3i\xi/2} \frac{\sin(3\xi/2)}{3\xi/2}. \end{aligned}$$

*Thus we have*

$$\phi(x) = \begin{cases} \frac{1}{3} & 0 \le x \le 3, \\ 0 & \textit{otherwise.} \end{cases}$$

*The functions* $\phi_{0,n}(x) = \phi(x-n)$ *are not orthonormal, but for any* $\alpha < \frac{1}{3}$, $m_0$ *has no zeros in* $[-\alpha\pi, \alpha\pi]$.

## 2.3 Compactly supported biorthogonal wavelets bases

Since the basic idea of biorthogonal multiwavelets bases of double multiresolution analysis is very similar to the one of orthonormal wavelet bases, we can mimic the construction of $\phi$ and $\psi$ in the orthonormal case.

Define the $2\pi$-periodic functions $m_0$, $m_1$, $\widetilde{m}_0$, and $\widetilde{m}_1$ as follows:

$$m_0(\xi) = \frac{1}{\sqrt{2}} \sum_n h_n \, e^{-in\xi}, \qquad m_1(\xi) = \frac{1}{\sqrt{2}} \sum_n g_n \, e^{-in\xi},$$

$$\widetilde{m}_0(\xi) = \frac{1}{\sqrt{2}} \sum_n \tilde{h}_n \, e^{-in\xi}, \qquad \widetilde{m}_1(\xi) = \frac{1}{\sqrt{2}} \sum_n \tilde{g}_n e^{-in\xi}.$$

where

$$g_n = (-1)^n \overline{\tilde{h}_{-n+1}}, \qquad \sum_n \tilde{h}_{n+2k} = \delta_{k,0},$$

$$g_n = (-1)^{n+1} \tilde{h}_{-n+1}, \qquad \tilde{g}_n = (-1)^{n+1} h_{-n+1}.$$

(For simplicity, we assume that only finitly many $h_n$ and $g_n$ are nonzero.)

**Definition 2.6** *Two scaling functions* $\phi$ *and* $\widetilde{\phi}$, *generating possibly different multiresolution analyses of* $L^2(\mathbb{R})$, *are said to be dual scaling functions if*

$$< \phi(\cdot - j), \widetilde{\phi}(\cdot - k) > := \int_{-\infty}^{+\infty} \phi(x-j) \overline{\widetilde{\phi}(x-k)} \, dx = \delta_{j,k}, \quad j,k \in \mathbb{Z}.$$

Now we define two scaling functions $\phi$ and $\widetilde{\phi}$ by

$$\widehat{\phi}(\xi) = (2\pi)^{1/2} \prod_{j=1}^{\infty} m_0(2^{-j}\xi)$$

and

$$\widehat{\widetilde{\phi}}(\xi) = (2\pi)^{1/2} \prod_{j=1}^{\infty} \widetilde{m}_0(2^{-j}\xi).$$

Obviously, the above infinite products can converge only if

$$m_0(0) = 1 = \widetilde{m}_0(0).$$

By the following lemma, borrowed from G. Deslauriers and S. Dubuc [13], we can see that $\phi$ and $\widetilde{\phi}$ are compactly supported.

**Lemma 2.1** *If*

$$\Gamma(\xi) = \sum_{n=N_1}^{N_2} \gamma_n \, e^{-in\xi} \quad \textit{with} \quad \sum_{n=N_1}^{N_2} \gamma_n = 1,$$

*then*

$$\prod_{j=1}^{\infty} \Gamma(2^{-j}\xi)$$

*is an entire function of exponential type. In particular, it is the Fourier transform of a distribution with support in* $[N_1, N_2]$.

PROOF. By the Paley–Wiener theorem for distributions, it is sufficient to prove that $\prod_{j=1}^{\infty} \Gamma(2^{-j}\xi)$ is an entire function of exponential type with bounds

$$\left| \prod_{j=1}^{\infty} \Gamma(2^{-j}\xi) \right| \leq C_1 (1 + |\xi|)_1^M \exp(N_1 |\Im \xi|) \qquad \text{for } \Im \xi \geq 0,$$

$$\left| \prod_{j=1}^{\infty} \Gamma(2^{-j}\xi) \right| \leq C_2 (1 + |\xi|)_2^M \exp(N_2 |\Im \xi|) \qquad \text{for } \Im \xi \geq 0,$$

for some $C_1$, $C_2$, $M_1$, $M_2$. For the detail, see [11], pp. 176–177. □

Also similar to the orthonormal scalar wavelet case, we define $\phi$ and $\widetilde{\phi}$ as

$$\widehat{\phi}(\xi) = e^{i\xi/2} \, \overline{\widetilde{m}_0(\xi/2 + \pi)} \, \widehat{\phi}(\xi/2)$$
$$\widehat{\widetilde{\phi}}(\xi) = e^{i\xi/2} \, \overline{m_0(\xi/2 + \pi)} \, \widehat{\widetilde{\phi}}(\xi/2).$$

Unlike the orthonormal case, where $|m_0(\xi)| \leq 1$ by (2.21) so that $|\widetilde{\phi}(\xi)| \leq 1$ automatically followed to ensure that $\phi \in L^2(\mathbb{R})$, there is no priori condition ensuring that $\widehat{\phi}$ and $\widehat{\widetilde{\phi}}$ are square integrable or bounded in the present case.

Conditions which ensure that the scaling functions have preassigned regularities are given in the following proposition taken from Proposition 4.9 in [3].

**Proposition 2.4** *Assume that both $m_0(\xi)$ and $\widetilde{m}_0(\xi)$ can be factored in the form*

$$m_0(\xi) = \left(\frac{1+e^{-i\xi}}{2}\right)^N f(\xi)$$

*and*

$$\widetilde{m}_0(\xi) = \left(\frac{1+e^{-i\xi}}{2}\right)^{\widetilde{N}} \tilde{f}(\xi),$$

*and suppose that for some $k$, $k_1 > 0$*

$$\begin{aligned} B_k &:= \sup_\xi |f(\xi)f(2\xi)\cdots f(2^{k-1}\xi)|^{1/k} < 2^{N-1/2}, \\ B_{k_1} &:= \sup_\xi |\tilde{f}(\xi)\tilde{f}(2\xi)\cdots \tilde{f}(2^{k_1-1}\xi)|^{1/k_1} < 2^{\widetilde{N}-1/2}. \end{aligned}$$

*Then $\phi$ and $\widetilde{\phi}$ are in $L^2(\mathbb{R})$ and*

$$\int_{-\infty}^{+\infty} \phi(x)\overline{\widetilde{\phi}(x-n)}\,dx = \delta_{n,0}.$$

PROOF. One introduces the functions

$$\begin{aligned} \hat{u}_n(\xi) &= (2\pi)^{-1/2}\left[\prod_{j=1}^{n} m_0(2^{-j}\xi)\right]\chi_{[-\pi,\pi]}(2^{-n}\xi) \\ \hat{\tilde{u}}_n(\xi) &= (2\pi)^{-1/2}\left[\prod_{j=1}^{n} \widetilde{m}_0(2^{-j}\xi)\right]\chi_{[-\pi,\pi]}(2^{-n}\xi) \end{aligned}$$

with support in $[-2^j\pi, 2^j\pi]$, and proves, under the conditions of the propositon, that

$$\lim_{n\to\infty} \hat{u}_n = \widehat{\phi}, \qquad \lim_{n\to\infty} \hat{\tilde{u}}_n = \widehat{\widetilde{\phi}}$$

in the $L^2$ sense. □

The above propositions ensure the square integrability of $\phi$ and $\widetilde{\phi}$ which constitute dual scaling functions, but we still need some extra conditions to obtain biorthogonal multiwavelets bases. The next theorem is taken from [3].

**Theorem 2.3** *Let $\{h_n\}_{n\in\mathbf{Z}}$ and $\{\tilde{h}_n\}_{n\in\mathbf{Z}}$ be finite real sequences satisfying*

$$\sum_{n\in\mathbf{Z}} h_n\tilde{h}_{n+2k} = \delta_{k,0},$$

*and define*

$$m_0(\xi) = 2^{-1/2} \sum_n h_n \, e^{-in\xi},$$

$$\widetilde{m}_0(\xi) = 2^{-1/2} \sum_n \tilde{h}_n \, e^{-in\xi},$$

$$\widehat{\phi}(\xi) = (2\pi)^{-1/2} \prod_{j=1}^{\infty} m_0(2^{-j}\xi),$$

$$\widehat{\widetilde{\phi}}(\xi) = (2\pi)^{-1/2} \prod_{j=1}^{\infty} \widetilde{m}_0(2^{-j}\xi).$$

*Suppose that, for some* $C > 0$, $\varepsilon > 0$,

$$|\widehat{\phi}(\xi)| \le C(1+|\xi|)^{-1/2-\varepsilon}, \qquad |\widehat{\widetilde{\phi}}(\xi)| \le C(1+|\xi|)^{-1/2-\varepsilon}. \tag{2.26}$$

*If we define*

$$\psi(x) = \sqrt{2} \sum_n (-1)^n \bar{h}_{-n+1} \phi(2x+n),$$

$$\widetilde{\psi}(x) = \sqrt{2} \sum_n (-1)^n h_{-n+1} \widetilde{\phi}(2x+n),$$

*then the functions*

$$\psi_{j,k}(x) = 2^{-j/2} \psi(2^{-j}x - k), \qquad j,k \in \mathbb{Z},$$

*constitute a frame in* $L^2(\mathbb{R})$. *Their dual frame is given by the the functions*

$$\widetilde{\psi}_{j,k}(x) = 2^{-j/2} \widetilde{\psi}(2^{-j}x - k), \qquad j,k \in \mathbb{Z},$$

*and, for any* $f \in L^2(\mathbb{R})$,

$$f(x) = \sum_{j,k \in \mathbb{Z}} < f, \widetilde{\psi}_{j,k} > \psi_{j,k}(x) = \sum_{j,k \in \mathbb{Z}} < f, \psi_{j,k} > \widetilde{\psi}_{j,k}(x),$$

*where the series converge strongly.*

*Moreover, the functions* $\psi_{j,k}$ *and* $\widetilde{\psi}_{j,k}$ *constitute a pair of dual Riesz bases, with*

$$< \psi_{j,k}, \widetilde{\psi}_{j',k'} >= \delta_{j,j'} \delta_{k,k'},$$

*if and only if*

$$\int \phi(x) \widetilde{\phi}(x-k) \, dx = \delta_{k,0}.$$

PROOF. The proof given in [3] is quite long and proceeds by means of seven lemmas. The first part mimicks the construction of $\phi$ and $\psi$ in the orthonormal case. Having constructed candidate functions $\psi$ and $\widetilde{\psi}$, one needs to show that they generate Riesz bases of wavelets. One obstruction is that there is no *a priori* estimate ensuring that $\widehat{\phi}$ and $\widehat{\widetilde{\phi}}$ are square integrable or bounded. For this purpose, one uses conditions (2.26). After some manipulation, one establishes the bounds

$$\sum_{j,k} | < f_1, \psi_{jk} > |^2 \leq C \|f_1\|^2, \qquad \text{for some } C \geq 0, \tag{2.27}$$

$$\sum_{j,k} | < f_2, \widetilde{\psi}_{jk} > |^2 \leq C \|f_2\|^2. \tag{2.28}$$

From these bounds, one derives the $L^2$-converge to $f \in L^2(\mathbb{R})$ of the limits

$$\lim_{J,K \to \infty} \sum_{|j| \leq J, |k| \leq K} < f, \psi_{jk} > \widetilde{\psi}_{jk} = \lim_{J,K \to \infty} \sum_{|j| \leq J, |k| \leq K} < f, \widetilde{\psi}_{jk} > \psi_{jk} = f.$$

Finally, one shows that $\psi_{jk}$ and $\widetilde{\psi}_{jk}$ constitute dual Riesz bases by establishing linear independence, that is

$$< \psi_{jk}, \widetilde{\psi}_{j'k'} > = \delta_{jj'} \delta_{kk'}.$$

This completes the discussion of the proof. □

We can also study the existence problem starting with $m_0$ and $m_1$.

Suppose the matrix $M$ is of the form

$$M = \begin{bmatrix} m_0(\xi) & m_1(\xi) \\ m_0(\xi + \pi) & m_1(\xi + \pi) \end{bmatrix},$$

then the necessary and sufficient condition for the existence of orthonormal wavelet bases is that $M$ be unitary, that is, $m_0$ and $m_1$ satisfy the identities

$$|m_0(\xi)|^2 + |m_0(\xi + \pi)|^2 = 1,$$
$$|m_1(\xi)|^2 + |m_1(\xi + \pi)|^2 = 1,$$

and

$$m_0(\xi)\overline{m_1(\xi)} + m_0(\xi + \pi)\overline{m_1(\xi + \pi)} = 0.$$

On the other hand, the necessary and sufficient condition for the existence of biorthogonal wavelet bases is that

$$\widetilde{h}(z)\overline{h}(z) + \widetilde{g}(z)\overline{g}(z) = 2,$$
$$\widetilde{h}(z)\overline{h}(-z) + \widetilde{g}(z)\overline{g}(-z) = 0,$$

where $z = e^{-i\xi}$.

This completes the basic theoretical steps in the construction of orthonormal wavelet bases and biorthogonal wavelet bases.

## 2.4 Construction of orthonormal wavelet bases

In this section, we provide a practical numerical technique for the construction of orthonormal wavelet bases.

From the theoretical steps for the construction of orthonormal wavelet bases, we see that the construction of $m_0$ is very important. Therefore, it is necessary to specify the construction of $m_0$ first. The Riesz Lemma tells us that we need only find a trigonometric polynomial $B(\xi)$ of order $M$ such that $|B(\xi)|^2 = A(\xi)$. We discuss this construction in three steps:

**Step 1.** Since

$$A(\xi) = \sum_{m=0}^{M} a_m \cos m\xi, \qquad a_m \in \mathbb{R},$$

it can be written as

$$A(\xi) = P_A(\cos\xi),$$

where $P_A$ is a polynomial of degree $M$ with real coefficients. $P_A$ can be factored as

$$P_A(c) = \alpha \prod_{j=1}^{M} (c - c_j),$$

where the zeros $c_j$ of $P_A$ appear either in complex conjugate pairs $c_j$, $\bar{c}_j$, or in real singlets.

On the other hand,

$$A(\xi) = e^{iM\xi} Q_A(e^{-i\xi}), \tag{2.29}$$

where $Q_A$ is a polynomial of degree $2M$. Let $z = e^{-i\xi}$, then $|z| = 1$; and

$$\begin{aligned} Q_A(z) &= z^M \alpha \prod_{j=1}^{M} \left( \frac{z + z^{-1}}{2} - c_j \right) \\ &= \alpha \prod_{j-1}^{M} \left( \frac{1}{2} z^2 - c_j z + \frac{1}{2} \right). \end{aligned} \tag{2.30}$$

**Step 2.** Consider

$$f(z) = \frac{1}{2} z^2 - c_j z + \frac{1}{2}.$$

There are two cases:

(i) If $c_j$ is real, then the zeros of $f(z)$ are $z = c_j \pm \sqrt{c_j^2 - 1}$.

1. For $|c_j| \geq 1$, these two real zeros are of the form $r_j$, $r_j{}^{-1}$, and they degenerate when $|c_j| = 1$.
2. For $|c_j| < 1$, the two zeros are complex conjugates with absolute value 1. These can be written in the form $e^{i\alpha_j}$, $e^{-i\alpha_j}$, and they correspond to the value $\xi$ such that $A(\xi) = 0$. Since $A \geq 0$, this kind of zeros must have even multiplicity.

(ii) If $c_j$ is not real, then we consider the polynormial

$$f(z) f'(z) = \left( \frac{1}{2} z^2 - c_j z + \frac{1}{2} \right) \left( \frac{1}{2} z^2 - \bar{c}_j z + \frac{1}{2} \right).$$

The zero of $f(z)f'(z)$ are $c_j \pm \sqrt{c_j{}^2 - 1}$ and $\bar{c}_j \pm \sqrt{\bar{c}_j^2 - 1}$.

1. For $|c_j| = 1$, these four zeros reduce to a pair of complex conjugate zeros with absolute value 1. Each of them has multiplicity two.
2. For $|c_j| \neq 1$, these four different zeros form a quadruplet $z_j$, $z_j{}^{-1}$, $\bar{z}_j$, $\bar{z}_j^{-1}$.

**Step 3.** Factoring $Q(z)$, we have

$$\begin{aligned} Q(z) &= \frac{1}{2} \alpha_M \left[ \prod_{l=1}^{L} (z - r_l)(z - r_l{}^{-1}) \right] \left[ \prod_{k=1}^{K} (z - e^{i\alpha_k})^2 (z - e^{-i\alpha_k})^2 \right] \\ &\quad \cdot \left[ \prod_{j=1}^{J} (z - z_j)(z - \bar{z}_j)(z - z_j{}^{-1})(z - \bar{z}_j^{-1}) \right]. \end{aligned}$$

Since $z$
$= e^{-i\xi}$ is on the unit circle , we have

$$|(e^{-i\xi} - z_0)(e^{-i\xi} - \bar{z}_0^{-1})| = |z_0|^{-1} |e^{-i\xi} - z_0|^2.$$

Substituting all the above into (2.29), we obtain

$$\begin{aligned} A(\xi) &= |A(\xi)| \\ &= |Q_A(e^{-i\xi})| \\ &= \left[\frac{1}{2}|\alpha_M| \prod_{l=1}^{L} |r_l|^{-1} \prod_{j=1}^{J} |z_j|^{-2}\right] \left[\prod_{l=-1}^{L} (e^{-i\xi} - r_l)\right]^2 \\ &\quad \cdot \left[\prod_{k=1}^{K} (e^{-i\xi} - e^{i\alpha_k})(e^{-i\xi} - e^{-i\alpha_k})\right]^2 \left[\prod_{j=1}^{J} (e^{-i\xi} - z_j)(e^{-i\xi} - \bar{z}_j)\right]^2 \\ &= |B(\xi)|^2. \end{aligned}$$

Consequently,

$$\begin{aligned} B(\xi) &= \left[\frac{1}{2}|\alpha_M| \prod_{l=1}^{L} |r_l|^{-1} \prod_{j=1}^{J} |z_j|^{-2}\right]^{1/2} \left[\prod_{l=1}^{L} (e^{-i\xi} - r_l)\right] \\ &\quad \cdot \left[\prod_{k=1}^{K} (e^{-i\xi} - e^{i\alpha_k})(e^{-i\xi} - e^{-i\alpha_k})\right] \left[\prod_{j=1}^{J} (e^{-i\xi} - z_j)(e^{-i\xi} - \bar{z}_j)\right] \\ &= \left[\frac{1}{2}|\alpha_M| \prod_{l=1}^{L} |r_l|^{-1} \prod_{j=1}^{J} |z_j|^{-2}\right]^{1/2} \left[\prod_{l=1}^{L} (e^{-i\xi} - r_l)\right] \\ &\quad \cdot \left[\prod_{k=1}^{K} (e^{-2i\xi} - 2e^{-i\xi}\cos\alpha_k + 1)\right] \left[\prod_{j=1}^{J} (e^{-2i\xi} - 2e^{i\xi} Re z_j + |z_j|^2)\right]. \end{aligned}$$

It is obvious that $B(\xi)$ is a trigonometric polynomial of order $M$ with real coefficients

We see from the above construction of $B$ that the polynomial $B$ is not unique. In fact, in each quadruplet we can choose any elements of the quadruplet, in each duplet we can choose either $r_l$ or $r_l^{-1}$ to make up $B$. In Daubechies' method, from the quadruplet, the two zeros with absolute value smaller than one are chosen, i.e.,

$z_j$ and $\bar{z}_j$ or $z_j^{-1}$ and $\bar{z}_j^{-1}$, and it will be seen later that such choice make the corresponding scaling functions and wavelet functions asymmetric except for the Haar wavelet. However, Lawton chose the two zeros from the quadruplet by replacing one zero of each conjugate pair by the reciprocal of its conjugate, i.e., $z_j$ and $z_j^{-1}$ or $\bar{z}_j$ and $\bar{z}_j^{-1}$. Such choice may make the corresponding scaling function and wavelet function symmetric. We will discuss the symmetry of Lawton's complex-valued scalar wavelet in the next chapter.

In general, there are no closed-form formulas for compactly supported $\phi(x)$ and $\psi(x)$. Nevertheless, if $\phi$ is continuous, we can compute $\phi(x)$ with arbitrarily high precision for any given $x$. Daubechies gave a fast algorithm called "Cascade Algorithm" to plot $\phi(x)$ and $\psi(x)$.

Before describing the cascade algorithm, we need two propositions.

**Proposition 2.5** *If $f$ is a continuous function on $\mathbb{R}$, then, for all $x \in \mathbb{R}$,*

$$\lim_{j\to\infty} 2^j \int f(x+y)\overline{\phi(2^j y)}\,dy = f(x).$$

*If $f$ is uniformly continuous, then this pointwise convergence is uniform as well. If $f$ is Hölder continuous with exponent $\alpha$,*

$$|f(x) - f(y)| \le c\,|x-y|^\alpha,$$

*then the convergence is exponentially fast in $j$:*

$$\left| f(x) - 2^j \int f(x+y)\overline{\phi(2^j y)}\,dy \right| \le c2^{-j\alpha}. \tag{2.31}$$

PROOF. All the assertions follow from the fact that $2^j\phi(2^j\cdot)$ is an "approximate $\delta$-function" as $j$ tends to $\infty$. More precisely,

$$\begin{aligned}
\left| f(x) - 2^j \int f(x+y)\overline{\phi(2^j y)}\,dy \right| &= \left| 2^j \int [f(x) - f(x+y)]\overline{\phi(2^j y)}\,dy \right| \\
&= \left| \int [f(x) - f(x+2^{-j}z)]\overline{\phi(z)}\,dz \right| \\
&\le \|\phi\|_{L^1} \cdot \sup_{|u|\le 2^{-j}R} |f(x) - f(x+u)|
\end{aligned}$$

(where we suppose that support $\phi \subset [-R, R]$). If $f$ is continuous, then this can be made arbitrarily small by choosing $j$ sufficiently large. If $f$ is uniformly continuous,

then the choice of $j$ can be made independently of $x$, and the convergence is uniform. If $f$ is Hölder continuous, then (2.31) follows immediately as well. This completes the proof. □

**Proposition 2.6** *If $\phi$ is Hölder continuous with exponent $\alpha$, then there exist $c > 0$ and $j_0 \in \mathbb{N}$ such that, for $j \geq j_0$,*

$$\|\phi - \eta_j^0\|_{L^\infty} \leq c\, 2^{-\alpha j}, \qquad \|\phi - \eta_j^1\|_{L^\infty} \leq c 2^{-\alpha j}, \tag{2.32}$$

*where $\eta_j^0(x)$ are the functions defined as piecewise constants on the intervals $\big[2^{-j}(n - 1/2), 2^{-j}(n + 1/2)\big)$, for $n \in \mathbb{N}$, such that $\eta_j^0(2^{-j}k) = 2^{j/2} < \phi, \phi_{-j,k} >$, and $\eta_j^1(x)$ are the functions defined as piecewise linear on $[2^{-j}n, 2^{-j}(n + 1))$, for $n \in \mathbb{Z}$, such that $\eta_j^1(2^{-j}k) = 2^{j/2} < \phi, \phi_{-j,k} >$.*

PROOF. The proof is taken from [11], pp. 205. Take any $x \in \mathbb{R}$. For any $j$, choose $n$ so that $2^{-j}n \leq x < 2^{-j}(n + 1)$. By the definition of $\eta_j^\varepsilon(x)$, $\eta_j^\varepsilon(x)$ is necessarily a convex linear combination of $2^{j/2} < \phi, \phi_{-j,n} >$ and $2^{j/2} < \phi, \phi_{-j,n+1} >$, whether $\varepsilon = 0$ or 1. On the other hand, if $j$ is larger than some $j_0$,

$$\begin{aligned} |\phi(x) - 2^{j/2} < \phi, \phi_{-j,n} > | &\leq |\phi(x) - \phi(2^{-j}n)| + |\phi(2^{-j}n) - 2^{j/2} < \phi, \phi_{-j,n} > | \\ &\leq c|x - 2^{-j}n|^\alpha + c2^{-j\alpha} \\ &\leq c2^{-j\alpha}; \end{aligned}$$

the same is true if we replace $n$ by $n+1$. It follows that a similar estimate holds for any convex combination, or $|\phi(x) - \eta_j^\varepsilon(x)| \leq c2^{-j\alpha}$. Here $c$ can be chosen independently of $x$, so that (2.32) follows. This completes the proof. □

In Proposition 2.5, if we take $f(x)$ as $\phi(x)$, and let $x$ be any dyadic rational, $x = 2^{-J}K$, then we have

$$\begin{aligned} \phi(x) &= \lim_{j\to\infty} 2^j \int \phi(2^{-J}K + y)\overline{\phi(2^j y)}\, dy \\ &= \lim_{j\to\infty} 2^j \int \phi(x)\overline{\phi(2^j x - 2^{j-J}K)}\, dy \\ &= \lim_{j\to\infty} 2^{j/2} < \phi, \phi_{-j,2^{j-J}K} > . \end{aligned}$$

Moverover,

$$|\phi(2^{-J}K) - 2^{j/2} < \phi, \phi_{-j,2^{j-J}K} > | \leq c2^{-2j\alpha}$$

whenever $j \geq j_0$, where $c$ and $j_0$ are dependent on $J$ or $K$. Therefore, we can get $\phi(x)$ at every dyadic rational $x$, and moreover get a sequence of functions approximating $\phi$ by interpolating the intervals with dyadic rational end points. Together with Proposition 2.6, it is clear that to get the scaling function $\phi$ with arbitrarily high precision, we need only compute the approximating function $\eta_j^\varepsilon$, where $\varepsilon = 0, 1$.

Now we state the 1-D cascade algorithm.

**Algorithm 2.1 (1-D Cascade Algorithm)** *Assume that $\phi$ is a compactly supported scaling function, which is continuous or Hölder continuous with exponent $\alpha$, and let $c_n^{-j} =< \phi, \phi_{-j,n} >$. Then the $c_m^{-j}$ are computed recursively by the convolution:*

$$c_n^0 = \delta_{0,n},$$
$$c_m^{-j} = \sum_n h_{m-2n} c_n^{-j+1}.$$

This algorithm provides a numerical approximation to the scaling function, and consequently, to the wavelets, to arbitrarily high precision.

## 2.5 Construction of biorthogonal wavelet bases

For biorthogonal wavelets, we can also use the cascade algorithm once we have a pair of dual filters, $m_0$ and $\widetilde{m}_0$. A. Karoui in his Ph.D. thesis [20] gave a method for constructing pairs of dual filters whose coefficients are given in parametric form. We shall skip the description of the method and the reader is referred to [20]

# Chapter 3

# Complex-Valued Wavelets

It was seen in Chapter 2 that real-valued wavelets with compact support cannot be symmetric except for the Haar wavelet. In signal analysis, symmetry is often desirable and sometimes necessary. Some years after the theory of real-valued orthonormal wavelet bases with compact support has been developed by Daubechies, Lawton [22] has shown that it is possible to achieve orthonormal and symmetric scaling functions and wavelets at the price of complex coefficients. Recently, J.-M. Lina and L. Gagnon [25] found that analysis based on complex-valued symmetric wavelets leads to a multiresolution form of the Laplacian operator and moreover that this property leads to new methods in image enhancement applications.

This chapter is organized as follows: firstly, we review Lawton's method to construct complex-valued wavelet bases; then we study some properties of these wavelets, comparing them with Daubechies' real-valued compactly supported wavelet bases.

## 3.1 Construction of complex-valued wavelets

Recall that the procedure for constructing real-valued compactly supported wavelet bases consists of three steps: firstly, we construct a scaling function $\phi$ which satisfies the two-scale relation

$$\phi(x) = \sum_n h_n \phi_{-1,n}(x) = \sqrt{2} \sum_n h_n \phi(2x - n) \tag{3.1}$$

and the normalization

$$\int \phi(x)\, dx = 1. \tag{3.2}$$

Secondly, we find a basic wavelet $\psi$ of the form

$$\psi(x) = \sum_n g_n \phi_{-1,n}(x) = \sqrt{2} \sum_n g_n \phi(2x - n) \tag{3.3}$$

where

$$g_n = (-1)^n \overline{h_{-n+1}}. \tag{3.4}$$

Finally, for any $j \in \mathbb{Z}$, the wavelet basis for $V_j$ is

$$\{\phi_{j,k};\ k \in \mathbb{Z}\} \cup \{\psi_{l,k};\ l < j,\ k \in \mathbb{Z}\}$$

where

$$\phi_{j,k} = 2^{-j/2}\phi(2^{-j}x - k), \qquad \psi_{j,k} = 2^{-j/2}\psi(2^{-j}x - k). \tag{3.5}$$

The key point to obtain the scaling function $\phi$ is the construction of $m_0$ by means of the Riesz Lemma.

The difference between the construction of real-valued wavelets and complex-valued wavelets lies in the construction of $m_0$. To simplify the discussion below, we first introduce a notation.

**Notation 3.1** *The "z-notation" consist in setting $z = e^{i\xi}$ in, say, a filter $m_0(\xi)$, for a point on the unit circle, and extend the value of $z$ to the complex plane.*

Let $N$ denote the number of vanishing moments of the wavelet $\psi(x)$, i.e., the support length of the frequency response $m_0(\xi)$ (or the support length of the corresponding scaling function). The $z$-transform $H(z) = \sum_n h_n z^{-n}$ of any real finite impluse response (FIR) conjugate quadrature filter (CQF) $h(\xi)$ of length $N$, has the factorization

$$H(z) = h_0 \left(1 + \frac{1}{z}\right)^{N/2} \prod_{l=1}^{L} \left(1 - \frac{r_l}{z}\right) \prod_{k=1}^{K} \left[z_k \left(1 - \frac{z_k}{z}\right)\left(1 - \frac{\overline{z}_k}{z}\right)\right], \tag{3.6}$$

where $2K$ is the number of complex roots and $L$ is the number of real distinct roots.

In the construction of real-valued wavelets, Daubechies chose the complex roots which satisfy $|z_k| \leq 1$, that is, all the complex roots lie inside or on the boundary of

the closed unit disk. However, this way of factorizing $H(z)$ is not unique. Lawton's method consists in replacing one zero of each conjugate pair by the reciprocal of its conjugate,

$$H_L(z) = h_0 \left(1 + \frac{1}{z}\right)^{N/2} \prod_{l=1}^{L} \left(1 - \frac{r_l}{z}\right) \prod_{k=1}^{K} \left[z_k \left(1 - \frac{z_k}{z}\right) \left(1 - \frac{\bar{z}_k^{-1}}{z}\right)\right]. \tag{3.7}$$

In the case $L = 0$, we have

$$H_L(z) = h_0 \left(1 + \frac{1}{z}\right)^{N/2} \prod_{k=1}^{K} \left[z_k \left(1 - \frac{z_k}{z}\right) \left(1 - \frac{z_k^{-1}}{z}\right)\right]. \tag{3.8}$$

To obtain the filters associated with $H_L(z)$, it suffices to multiply their coefficients by $\sqrt{2}$.

## 3.2 Properties of complex-valued wavelets

In the previous section, we reviewed the construction of complex-valued wavelets. In this section, we shall study the properties of complex-valued wavelets and compare them with real-valued wavelets. For convenience, we let $\phi_L$ and $\phi_D$ denote the scaling functions of complex-valued wavelets and real-valued wavelets, respectively, and $\psi_L$ and $\psi_D$ denote complex-valued and real-valued wavelets, respectively.

### Compactness of the scaling function $\phi_L$

For a fixed integer $N$, the scaling function $\phi_L$ has the same vanishing moments as $\phi_D$ because $\phi_L$ and $\phi_D$ have the same filter or mask, that is,

$$m_0(\xi) = \left(\frac{1 + e^{-i\xi}}{2}\right)^N \mathcal{L}(\xi), \qquad \text{where } \mathcal{L} \text{ is a trigonometric polynomial.}$$

Thus $\phi_L$ can have compact support and consequently $\psi_L$ has a compact support in the interval $[-J, J+1]$ for some integer $J$, i.e., $h_k \neq 0$ for $k = -J, -J+1, \ldots, J, J+1$.

### Orthogonality of the translates $\phi_L(x-k)$

In the case of real-valued wavelets, the condition of orthogonality of $\phi_D(x-k)$ defines in a large sense the Daubechies wavelets. To state the condition in the case of complex-

valued wavelets, we rewrite the $z$-transform $H$ in the form

$$H(z) = \sum_{n=-J}^{J+1} h_n z^{-n} \tag{3.9}$$

with

$$H(1) = 1. \tag{3.10}$$

Then as the real-valued case, the orthogonality of $\{(\phi_L)_{0,k}\}_{k\in\mathbb{Z}}$ is equivalent to the relation

$$P(z) - P(-z) = z, \tag{3.11}$$

where the polynomial $P(z)$ is defined as

$$P(z) = zH(z)\overline{H(z)}. \tag{3.12}$$

**Accuracy of the approximation**

It has been known that in the multiresolution approximating process, any function $f$ in $V_j$ can be approximated as

$$f(x) \approx \sum_{k\in\mathbf{Z}} c_k^j \phi_{j,k}(x) \tag{3.13}$$

where

$$c_k^j = < f, \phi_{j,k} > . \tag{3.14}$$

To maximize the regularity of the functions generated by the scaling function $\phi$, we require that the first $J$ moments of the wavelet vanish, in other words, in terms of $H(z)$, we require that

$$H'(-1) = H''(-1) = \ldots = H^{(J-1)}(-1) = 0. \tag{3.15}$$

The real-valued wavelets are the real polynomial solutions of (3.11) and (3.15) with filters of length $N = 2J + 2$.

### Symmetry

As claimed by Lawton, only complex-valued solutions of $\phi$ and $\psi$ can achieve compact support and symmetry at the same time with $N/2$ odd, that is, $J$ even ($N/2 = J+1$). By the construction (3.7) of Lawton's wavelets, we have

$$L + 2K = N/2 - 1. \tag{3.16}$$

If $N/2$ is even, then $L \neq 0$, which means that $H(z)$ has real roots and it is not possible to construct a symmetric filter. Thus we cannot get symmetric scaling functions and symmetric wavelets.

On the other hand, if $N/2$ is odd, then all roots of $H(z)$ are nonreal, therefore $L = 0$ and a symmetric filter can be constructed.

The condition of symmetry on the filter means

$$h_n = h_{1-n}, \qquad -J \leq n \leq J+1. \tag{3.17}$$

In the $z$-transform, this condition can be expressed as

$$H(z) = zH(z^{-1}). \tag{3.18}$$

J.-M. Lina and M. Mayrand [26] described the first solutions in terms of a parameter $J$, ($J = 0, 1, \ldots, 8$), by using parametrized solutions of equations (3.11), (3.14) and (3.18). These solutions have also been studied by an inspection of the roots of some polynomials which satisfy (3.11). Such polynomials are defined by

$$P_J(z) = \left(\frac{1+z}{2}\right)^{2J+2} p_J(z^{-1}), \tag{3.19}$$

where

$$p_J(z) = \sum_{j=0}^{2J} r_j (z+1)^{2J-j} (z-1)^j \tag{3.20}$$

with

$$r_{2j} = (-1)^j 2^{-2J} \begin{pmatrix} 2J+1 \\ j \end{pmatrix},$$
$$r_{2j+1} = 0,$$

for $j = 0, 1, \ldots, J$. It is easy to show that $P_J(z)$ satisfies (3.11).

The $2J$ roots display the symmetry since the conjugate inverse of a root is also a root, and furthermore, there are no roots having unit modulus.

Suppose the roots inside the unit circle, i.e., $|z_k| < 1$, are denoted by $z_k$ for $k = 1, 2, \ldots, J$, and $\bar{z}^k = z_{J+1-k}$, then

$$P_J(z) = \prod_{k=1}^{J} \left( \frac{z - z_k}{1 - z_k} \right) \prod_{k=1}^{J} \left( \frac{z - \bar{z}_k^{-1}}{1 - \bar{z}_k^{-1}} \right). \tag{3.21}$$

The $z$-transform $H(z)$ can then be written as

$$H(z) = \left( \frac{1+z}{2} \right)^{1+J} p(z^{-1}) \tag{3.22}$$

with

$$p(z) = \prod_{m \in R} \left( \frac{z - z_m}{1 - z_m} \right) \prod_{n \in R'} \left( \frac{z - \bar{z}_n^{-1}}{1 - \bar{z}_n^{-1}} \right),$$

where $R$ and $R'$ are two arbitrary subsets of $\{1, 2, \ldots, J\}$ . Due to the spectral factorization (3.12) of $P(z)$, we have

$$p_J(z) = z^J p(z^{-1}) \overline{p(z)},$$

and this leads to the following constraint on $R$ and $R'$: $R \bigcap R' = \emptyset$, i.e.,

$$k \in R \Leftrightarrow k \notin R'. \tag{3.23}$$

This selection of the roots satisfies the first three properties. For real-valued Daubechies wavelets, all the real solutions for $h_k$ are also derived from the constraint (3.23). This is equivalent to considering

$$k \in R \Leftrightarrow J + 1 - k \in R \text{ and } k \notin R'. \tag{3.24}$$

One instance of this condition is to let $R = \{1, 2, \ldots, J\}$ and $R' = \emptyset$; this corresponds to the Daubechies wavelets with the highest number of vanishing moments $N = 2J+2$, that is, the "least asymmetric" wavelets. However, the symmetric complex-valued wavelets are obtained by another subset of solutions of (3.23). This subset corresponds to

$$k \in R \Leftrightarrow J + 1 - k \in R' \text{ and } k \notin R'. \tag{3.25}$$

We notice that conditions (3.24) and (3.25) are incompatible. Therefore, only complex-valued wavelets can be symmetric.

The complex-valued wavelets share the usual properties of the real-valued wavelets and they can be symmetric. Besides that, the complex-valued wavelets have an unexpected analytic structure that relates the real and imaginary parts of the scaling functions. In particular, suppose that the complex scaling function and wavelet are written as

$$\phi(x) = h(x) + ig(x), \qquad \psi(x) = \omega(x) + i\nu(x),$$

where $h$, $g$, $\omega$ and $\nu$ are real functions.

Using the Fourier representation of these four real functions, $h(x)$, $g(x)$, $\omega(x)$ and $\nu(x)$, it can be shown that for small values of $J$ ($J < 12$), the complex scaling function and the wavelet of the multiresolution analysis for those symmetric complex-valued wavelets can be written as

$$\begin{cases} \phi(x) \simeq h(x) + i\alpha\partial_x^2 h(x), \\ \\ \psi(x) \simeq \omega(x) + ik\omega(x) + i\beta\partial_x^2\omega(x). \end{cases} \tag{3.26}$$

These identities are verified in the interval $[0, \pi]$ when they are written in the Fourier representation.

For $J > 10$, higher derivative terms in $h(x)$ become non negligible. Obviously, the two real functions $h(x)$ and $\omega(x)$ are a genuine scaling function and a true wavelet only in the case of a real multiresolution analysis ($\alpha = \beta = k = 0$). In the complex case, $h(x)$ (the real part of the scaling function) and $\omega(x)$ (the real part of the wavelet) are still endowed with interesting properties. Indeed, $h(x)$ is a good smoothing function since we can easily verify that

$$\int \overline{\phi(x)}\, dx = 1,$$

$$\int \overline{\phi(x)} \left(x - \frac{1}{2}\right)^m dx = 0, \qquad \text{for } m = 1, 2 \text{ and } 3.$$

Moreover, $\omega(x)$ is an "admissible wavelet" with $J$ vanishing moments.

The parameters $\alpha$, $\beta$ and $k$ in (3.26) can be computed directly from the filter coefficients $h_n$ by using the first nonvanishing moments of $\phi(x)$ and $\psi(x)$. Denoting by

$$\gamma_i = \int \overline{\phi(x)} x^i\, dx, \qquad \Gamma_i = \int \overline{\psi(x)} x^i\, dx,$$

we have

$$\gamma_i = \frac{1}{2^i - 1} \sum_{j=0}^{i-1} m_{i-j}\gamma_j, \quad \text{with } m_k = \textstyle\sum_{n=-J}^{J+1} n^k \overline{h_n} \text{ and } \gamma_0 = 1,$$

and

$$\Gamma_i = \frac{1}{2^i} \sum_{j=0}^{i} l_{i-j}\gamma_j, \quad \text{with } l_k = \textstyle\sum_{n=-J}^{J+1} n^k \overline{b_n}.$$

Straightforward integrations by parts lead to

$$\alpha = -\frac{1}{2}\Im(\gamma_2), \quad \beta = -\frac{k\Re(\Gamma_{J+3}) + \Im(\Gamma_{J+3})}{(J+3)(J+2)\Re(\Gamma_{J+1})} \quad \text{and} \quad k = -\frac{\Im(\Gamma_{J+1})}{\Re(\Gamma_{J+1})}.$$

This property can help in interpreting redundant descriptions of signals.

This theory is beyond the scope of this thesis and we refer the readers to [25], [26], [27], [28]. In these references, among other results, one finds two applications in image processing: enhancement and restoration of images. In both cases, the efficiency of this multiscale representation relies on the information encoded in the phase of the complex wavelet coefficients.

# Chapter 4

# Multiwavelets

It is well known that real-valued wavelets can not be compactly supported and symmetric at the same time except for the Haar wavelet. Complex-valued wavelets can achieve compact support and symmetry simultaneously, but complex-valued coefficients produce some redundancy in describing signals. Therefore, in the majority of cases, the three properties of symmetric scaling functions and wavelets, orthogonality and real coefficients are desirable. Recent studies have shown that these three properties can be achieved simultaneously if the coefficients of the filters become matrices and not scalars. The resulting scaling function, $\Phi$, and wavelet, $\Psi$, are vectors, and have been called multiwavelets.

Multiwavelets open new possibilities. Besides symmetry, they can have shorter support, with more vanishing moments, than scalar wavelets. Short support is necessary in some applications. Filters with short support have simple implementations and achieve good time localizations. However, they do not have good frequency domain behavior. The frequency responses are poor and the frequency localization is not good either.

In this chapter, we study some multiwavelets and compare them with complex wavelets. The organization of this chapter is as follows: the common characters are introduced first, then three kinds of multiwavelets are studied and a brief comparison of different wavelets is made.

## 4.1 Multiwavelet theory

The theory of multiwavelets is not a straightforward generalization of the theory of scalar wavelets. The main difference is that, in general, matrix multiplication is not commutative. A number of results on scalar filter banks are valid only because multiplication of scalar quantities is commutative.

The following results are taken mainly from [5], pp. 186–204.

First, we start with a notation, which will be used in later discussion.

**Notation 4.1** *Let $H_0(\xi)$, $H_1(\xi)$ denote the lowpass and highpass analysing multifilters and $G_0(\xi)$, $G_1(\xi)$ denote the lowpass and highpass synthesizing multifilters, respectively, of a two-channel multifilter bank, i.e.,*

$$H_0(\xi) = \frac{1}{\sqrt{2}} \sum_n h_n^{(0)} e^{-in\xi}, \qquad H_1(\xi) = \frac{1}{\sqrt{2}} \sum_n h_n^{(1)} e^{-in\xi},$$
$$G_0(\xi) = \frac{1}{\sqrt{2}} \sum_n g_n^{(0)} e^{-in\xi}, \qquad G_1(\xi) = \frac{1}{\sqrt{2}} \sum_n g_n^{(1)} e^{-in\xi}, \tag{4.1}$$

*where $h_n^{(i)}$, $g_n^{(i)}$, $i = 0, 1$, are $2 \times 2$ matrices. Let $H_0(z)$, $H_1(z)$, $G_0(z)$, $G_1(z)$ denote the z-transform of $H_0(\xi)$, $H_1(\xi)$, $G_0(\xi)$, $G_1(\xi)$, respectively, that is,*

$$H_0(z) = \sum_n h_n^{(0)} z^{-n}, \qquad H_1(z) = \sum_n h_n^{(1)} z^{-n},$$
$$G_0(z) = \sum_n g_n^{(0)} z^{-n}, \qquad G_1(z) = \sum_n g_n^{(1)} z^{-n}, \tag{4.2}$$

*Then, following standard terminology, we call $H_i(z)$, $G_i(z)$, $i = 0, 1$, matrix Laurent polynomials, since they can include negative powers of $z$.*

With the above notation, the orthogonality of multiwavelet filters is characterized by the identities

$$H_0(z)\widetilde{H}_0(z) + H_0(-z)\widetilde{H}_0(-z) = I, \tag{4.3}$$
$$H_1(z)\widetilde{H}_1(z) + H_1(-z)\widetilde{H}_1(-z) = I, \tag{4.4}$$
$$H_0(z)\widetilde{H}_1(z) + H_0(-z)\widetilde{H}_1(-z) = 0, \tag{4.5}$$
$$H_1(z)\widetilde{H}_0(z) + H_1(-z)\widetilde{H}_0(-z) = 0, \tag{4.6}$$

where $\widetilde{H}_i$ is defined as $\widetilde{H}_i(z) = H_{i*}^T(z^{-1})$, where the subscript * denotes complex conjugation of the coefficients. In general, the product of $H_i(z)$ and $\widetilde{H}_i(z)$, as well as $H_{1-i}(z)$ and $\widetilde{H}_{1-i}(z)$, does not commute. The orthogonality in the time domain is given by the relations

$$< h_0(n), h_0^T(n+2k) > = \delta_k I, \tag{4.7}$$

$$< h_1(n), h_1^T(n+2k) > = \delta_k I, \tag{4.8}$$

$$< h_0(n), h_1^T(n+2k) > = 0. \tag{4.9}$$

To discuss more deeply the properties possessed by multiwavelets, we need some definitions.

**Definition 4.1** *A filter with filter coefficients $\alpha_n$ is called linear phase if the phase of the function $\alpha(\xi) = \sum_n \alpha_n e^{-in\xi}$ is a linear function of $\xi$, i.e., for some $l \in \mathbb{Z}$,*

$$\alpha(\xi) = |\alpha(\xi)| e^{-il\xi}.$$

*This means that the coefficients $\alpha_n$ are symmetric about $l$, i.e., $\alpha_n = \alpha_{2l-n}$.*

**Definition 4.2** *A multifilter is called a linear-phase multifilter if and only if all of its components are linear-phase polynomials.*

**Definition 4.3** *A zero-phase multifilter $H(z)$ is called a half-band multifilter if and only if*

$$H(z) + H(-z) = cI, \qquad \text{where } c \neq 0.$$

**Definition 4.4** *A zero-phase multifilter $H(z)$ is a polynomial matrix, and its auto-correlation (or spectral) matrix $A$ is defined as*

$$A(z) = H(z)\widetilde{H}(z) = H(z)H_*^T(z^{-1}).$$

From Definition 4.3, we should notice that not all elements of a half-band multi-filter are half-band polynomials themselves, but only those that are along the main diagonal must be half-band polynomials and the others must contain only odd powers of $z$.

From Definition 4.4, we have the following proposition.

**Proposition 4.1** *A necessary condition to have an orthogonal multifilter bank is that the product filter $P(z) = H_0(z)\widetilde{H}_0(z)$ be a half-band autocorrelation matrix.*

PROOF. This result follows from Definitions 4.3 and 4.4 and relation (4.7). □

**Remark 4.1** *(i) In the case of scalar wavelet filter banks, the condition of Proposition 4.1 is not only necessary, but also sufficient. However, in general, this condition is only necessary in the case of vector filter banks because matrix multiplication is noncommutative.*

*(ii) In the scalar case, the step from the scaling function to the wavelet is automatic, but this automatic method fails in the multiwavelet case because the filter coefficients are matrices. Thus we need some other methods. Proposition 4.1 will offer a general design method to get multifilter banks. If we start with any linear-phase half-band autocorrelation matrix, then we can obtain an orthogonal perfect-reconstruction multifilter bank by matrix spectral factorization.*

**Condition 4.1 (Eigenvalue condition)** *Let $\lambda_1, \lambda_2, \ldots, \lambda_n$ be the eigenvalues of an $n \times n$ matrix $M$. The matrix is said to satisfy the eigenvalue condition if $\lambda_1 = 1$ is a simple eigenvalue and $|\lambda_i| < 1$, $i = 2, \ldots, n$.*

The following proposition has been established by A. Cohen, I. Daubechies and G. Plonka [4] and C. Heil and D. Colella [18].

**Proposition 4.2** *Suppose the multiscaling functions satisfies the following dilation equation in the frequency domain*

$$\widehat{\Phi}(\xi) = H_0(\xi/2)\widehat{\Phi}(\xi/2). \tag{4.10}$$

*If $H_0(0)$ satisfies the Eigenvalue Condition 4.1, then the solution to (4.10) is unique.*

PROOF. Assuming that $H_0(\xi)$ is a Laurent polynomial, one extends $H_0(\xi)$ to the complex plane, $\zeta = \xi + i\eta$. The result follows from estimates on

$$\|H_0(2^{-1}\zeta)\cdots H_0(2^{-n}\zeta)\|$$

in the complex plane. For the detail, see [4]. □

**Remark 4.2** *In particular [34], if* $\widehat{\Phi}(0) \neq 0$, *the solution* $\Phi(x)$ *is determined uniquely up to a constant factor. In fact, if*

$$H_0^{\infty}(\xi) = \prod_{j=1}^{\infty} H_0(\xi/2^j),$$

*then*

$$\widehat{\Phi}(\xi) = cH_0^{\infty}(\xi)\boldsymbol{b}$$

*where* $\boldsymbol{b}$ *is an arbitrary vector satisfying* $\boldsymbol{v}_1^T\boldsymbol{b} = 1$ *for the left eigenvector* $\boldsymbol{v}_1$ *of* $H_0(0)$ *associated to the eigenvalue* $\lambda_1 = 1$.

We note that the weaker condition $\boldsymbol{v}_1^T\boldsymbol{b} \neq 0$ is sufficient.

Now we describe the general design in more detail.

Suppose $P(z)$ is the product filter of an orthogonal multifilter bank, that is,

$$P(z) = H_0(z)H_0^T(z^{-1}) \tag{4.11}$$

$$= \begin{bmatrix} P^{11}(z) & P^{12}(z) \\ P^{21}(z) & P^{22}(z) \end{bmatrix}. \tag{4.12}$$

Moreover, suppose that $P(z)$ is a half-band multifilter, i.e.,

$$P(z) + P(-z) = I. \tag{4.13}$$

Then by matrix spectral factorization, we can find $H_0(z)$ such that

$$H_0(z)\widetilde{H}_0(z) = P(z). \tag{4.14}$$

An efficient matrix spectral factorization algorithm necessarily can handle zeros on the unit circle. For instance, the matrix spectral factorization due to Youla and Kazanjian [43] can handle zeros on the unit circle. The detailed procedure is described in [5].

A very important requirement of the design is that

$$\det P(z) = z^{K/2}(1 + z^{-1})^K Q(z), \tag{4.15}$$

where $K$ is any even number specified in advance and $Q(z)$ is a linear-phase polynomial in $z^{-1}$. Note that $K$ must be an even number because

$$\begin{aligned} \det P(z) &= \det H_0(z) \det \widetilde{H}_0(z) \\ &= |\det H_0(z)|^2, \end{aligned} \tag{4.16}$$

and only $K/2$ zeros are assigned to $\det H_0$. Moreover, the product multifilter $P(z)$ must be a Hermitian matrix, i.e.,

$$P\left(e^{i\xi}\right) = \overline{P^T\left(e^{i\xi}\right)}. \tag{4.17}$$

After discussing the general design, we turn to the general properties of multiwavelet bases. As in the case of scalar wavelet bases, we write the equivalent "lowpass" and "highpass" filters after $i$ iterations as

$$H_0^i(z) = H_0(z^{2^i})H_0(z^{2^{i-1}})\cdots H_0(z) \tag{4.18}$$

$$H_1^i(z) = H_1(z^{2^i})H_0(z^{2^{i-1}})\cdots H_0(z), \tag{4.19}$$

where the order of multiplication is important.

If for some two-vector $\mathbf{e}$ and under special conditions, the two functions

$$f_{1,n}^i = h_{0,n}^i \mathbf{e}, \qquad f_{2,n}^i = h_{1,n}^i \mathbf{e}, \tag{4.20}$$

converge to a pair of continuous functions, $\Phi(x)$ and $\Psi(x)$,

$$\Phi(x) = \lim_{i\to\infty} f_{1,n}^i, \qquad \Psi(x) = \lim_{i\to\infty} f_{2,n}^i, \tag{4.21}$$

then we say that the multifilter bank is regular. The limit functions $\Phi(x)$ and $\Psi(x)$ are the multiscaling function and multiwavelet, respectively:

$$\Phi(x) = \sqrt{2}\sum_n h_{0,n}\Phi(2x-n), \tag{4.22}$$

$$\Psi(x) = \sqrt{2}\sum_n h_{1,n}\Phi(2x-n), \tag{4.23}$$

$$\widehat{\Phi}(\xi) = \prod_{j=1}^{\infty} H_0(\xi/2^j), \tag{4.24}$$

$$\widehat{\Psi}(\xi) = H_1(\xi)\prod_{j=1}^{\infty} H_0(\xi/2^j). \tag{4.25}$$

Hence

$$\widehat{\Phi}(\xi) = H_0(\xi/2)\widehat{\Phi}(\xi/2). \tag{4.26}$$

When $\xi = 0$, (4.26) becomes

$$\widehat{\Phi}(0) = H_0(0)\widehat{\Phi}(0). \tag{4.27}$$

Thus,

$$(H_0(0) - I)\widehat{\Phi}(0) = 0, \tag{4.28}$$

where $I$ is the $2 \times 2$ identity matrix.

To obtain a non-trivial solution of (4.28), we need to have

$$\det(H_0(0) - I) = 0. \tag{4.29}$$

Equation (4.27) shows that $H_0(0)$ has eigenvalue 1 (this corresponds to $m_0(0) = 1$ in the scalar case).

In [11], Daubechies gave two methods to estimate the regularity of scalar wavelets. Unfortunately, not all scalar approaches can be generalized to the multiwavelet case. Shen [34] has characterized the regularity of multiwavelets by means of necessary and sufficient conditions on the filters, using the properties of transition operators. This is beyond the scope of this thesis.

G. Strang and V. Strela [37] gave an approach to test the accuracy of multiwavelets. Their method consits in forming an infinite block matrix, consisting of the filter coefficients (which are matrices), shifted by 2 in adjacent rows:

$$\begin{bmatrix} \cdots & & & & & & & & \\ & h_3 & h_2 & h_1 & h_0 & & & & \\ & & & h_3 & h_2 & h_1 & h_0 & & \\ & & & & & h_3 & h_2 & h_1 & h_0 \\ & & & & & & & & \cdots \end{bmatrix}.$$

If this matrix has eigenvalues $1, \frac{1}{2}, \cdots, \left(\frac{1}{2}\right)^N$, then the multiwavelets have $N$ vanishing moments. This method is a straight extension of similar result for the scalar wavelet case.

From (4.18), we have

$$\det H_0^{\infty}(z) = \lim_{i \to \infty} \det H_0(z^{2^{i-1}}) \det H_0(z^{2^{i-1}}) \cdots \det H_0(z). \tag{4.30}$$

This relation clearly implies the following proposition.

**Proposition 4.3** *A necessary condition to obtain multiwavelets with $N$ vanishing moments is that* $\det H_0(z)$ *has a zero of order $N$ at $z = -1$.*

Up to now, we have discussed the general multiwavelet theory and the general design of multifilters. In the next section, we shall study three kinds of multiwavelets.

## 4.2 Examples of multiwavelets

After considering the existence and discussion of orthonormal scalar wavelets, people began discussing multiwavelets. The first multiscaling function was constructed by Geronimo, Hardin and Massopust [15]. Donavan, Geronimo, Hardin and Massopust [14] constructed the corresponding multiwavelet. Strang and Strela [36] have constructed the D-G-H-M multiwavelet and other multiwavelets [37]. Many other people studied multiwavelets such as Daubechies [11], [12], Ashino, Nagase and Vaillancourt [1], and Cooklev [5], [6], [7], [8], [9], and others. In this section, we shall study multiscaling functions and multiwavelets constructed by the above quoted persons.

### Donavan-Geronimo-Hardin-Massopust multiwavelet

The G-H-M multiscaling function and D-G-H-M multiwavelet have been constructed by Geronimo, Hardin and Massopust [15] and Donavan, Geronimo, Hardin and Massopust [14], respectively, by means of factal interpolation functions. The D-G-H-M multiwavelet has also been constructed by Strang and Strela [36] by means of algebraic methods in the time domain. Here we shall follow the latter method.

The G-H-M scaling functions can be characterized by the following properties:

1. Symmetry: The first obvious character is that the two scaling functions $\phi_1$ and $\phi_2$ are symmetric functions (see Fig. 4.1 below), which satisfy

$$\phi_1(x) = \phi_1(1-x), \qquad \phi_2(x) = \phi_2(2-x).$$

2. Short support: It is a unique character of the G-H-M scaling functions. The functions $\phi_i$, $i = 1, 2$, vanish outside $[0, i]$.

3. Second-order accuracy: The two scaling functions can produce the hat function exactly:

$$\frac{1}{\sqrt{2}}\phi_1(x) + \frac{1}{\sqrt{2}}\phi_1(x-1) + \phi_2(x) = \begin{cases} x, & 0 \le x < 1, \\ 2-x, & 1 \le x \le 2, \end{cases}$$

that is, a combination of the translation of $\phi_1(x)$ and $\phi_2(x)$ yields the functions 1 and $x$. This establishes two vanishing moments for the new wavelets which will be orthogonal to the functions 1 and $x$, i.e.,

$$\int 1 \cdot \psi_i(x)\, dx = 0, \qquad i = 1, 2,$$

$$\int x\, \psi_i(x)\, dx = 0, \qquad i = 1, 2.$$

Therefore, the order of approximation is 2.

4. Orthogonality: The translates of the two scaling functions,

$$\{\phi_1(x-k)\}_{k\in\mathbf{Z}}, \qquad \{\phi_2(x-k)\}_{k\in\mathbf{Z}},$$

are all mutually orthogonal, that is,

$$\int \phi_i(x-k)\phi_j(x-l)\, dx = \delta_{i-j}\delta_{k-l}, \qquad i = 1, 2,\ j \in \mathbb{Z}. \tag{4.31}$$

Once the scaling functions have been found with the above four properties, the next step is to construct the corresponding orthonormal multiwavelets from the scaling functions. This step is not automatic since the filter coefficients are matrices. Strang and Strela considered the multiscale relations

$$\Phi(x) = \begin{bmatrix} \phi_1(x) \\ \phi_2(x) \end{bmatrix} = \sum_{k\in\mathbf{Z}} h_k \begin{bmatrix} \phi_1(2x-k) \\ \phi_2(2x-k) \end{bmatrix},$$

$$\Psi(x) = \begin{bmatrix} \psi_1(x) \\ \psi_2(x) \end{bmatrix} = \sum_{k\in\mathbf{Z}} g_k \begin{bmatrix} \phi_1(2x-k) \\ \phi_2(2x-k) \end{bmatrix},$$

where $h_k$ and $g_k$ are matrix coefficients, and $g_k$ are obtained as the solution of linear and quadratic equations, whose solution was first computed by Mathematica. The key point of their method is to find a paraunitary matrix $P(z)$, that is, a matrix Laurent polynomial which is unitary on the unit circle $|z| = 1$. Then the scaling

functions come from one half of the matrix and the wavelets come from the other half. More specifically, let $L$ be the matrix consisting of the low-pass coefficients:

$$L = \frac{1}{\sqrt{2}} \begin{bmatrix} \cdots & & & & & & & \\ & h_0 & h_1 & h_2 & h_3 & & & \\ & & & h_0 & h_1 & h_2 & h_3 & \\ & & & & & & & \cdots \end{bmatrix}.$$

Now $L$ is a block Toeplitz matrix where

$$h_0 h_0^T + h_1 h_1^T + h_2 h_2^T + h_3 h_3^T = 2I,$$
$$h_0 h_2^T + h_1 h_3^T = 0;$$

thus, half of the rows in $L$ satisfies $LL^T = I$.

Then construct a new matrix of the form

$$\begin{bmatrix} L \\ B \end{bmatrix} = \frac{1}{\sqrt{2}} \begin{bmatrix} h_0 & h_1 & h_2 & h_3 & & \\ & & h_0 & h_1 & h_2 & h_3 \\ \cdot & \cdot & \cdot & \cdot & \cdot & \cdot \\ g_0 & g_1 & g_2 & g_3 & & \\ & & g_0 & g_1 & g_2 & g_3 \end{bmatrix}.$$

Since $LL^T = I$, to obtain orthogonal multiwavelets, it remains to require that $LB^T = 0$ and $BB^T = I$. After some matrix transformation and calculation, we get a paraunitary matrix $P(z)$,

$$P(z) = \begin{bmatrix} L(z) \\ B(z) \end{bmatrix} = \begin{bmatrix} L(1) \\ B(1) \end{bmatrix} U(z), \tag{4.32}$$

where

$$P(z) = P_0 + P_1 z^{-1}$$

and

$$P(z)\widetilde{P}(z) = 2I$$

with

$$P_0 = \begin{bmatrix} h_0 & h_1 \\ g_0 & g_1 \end{bmatrix}, \qquad P_1 = \begin{bmatrix} h_2 & h_3 \\ g_2 & g_3 \end{bmatrix}.$$

Here, $U(z)$ has a specific form given by Vaidyanathan [40] and $\widetilde{P}(z)$ denotes the conjugate transpose of $P(1/\bar{z})$.

From (4.32), we can get $B(z)$ from the product $B(1)U(z)$. This gives the coefficients of the highpass filter, and consequently, the orthogonal multiwavelets follow. A more detailed construction is found in [36], [37].

The G-H-M lowpass and D-G-H-M highpass multifilters in the $z$-notation are

$$H_0^G(z) = \frac{1}{10}\begin{bmatrix} 6 & 8\sqrt{2} \\ -1/\sqrt{2} & -3 \end{bmatrix} + \frac{1}{10}\begin{bmatrix} 6 & 0 \\ 9/\sqrt{2} & 10 \end{bmatrix} z^{-1} + \frac{1}{10}\begin{bmatrix} 0 & 0 \\ 9/\sqrt{2} & -3 \end{bmatrix} z^{-2} + \frac{1}{10}\begin{bmatrix} 0 & 0 \\ -1/\sqrt{2} & 0 \end{bmatrix} z^{-3}$$

$$H_1^G(z) = \frac{1}{10}\begin{bmatrix} -1/\sqrt{2} & -3 \\ 1 & 3\sqrt{2} \end{bmatrix} + \frac{1}{10}\begin{bmatrix} 9/\sqrt{2} & -10 \\ 9 & 0 \end{bmatrix} z^{-1} + \frac{1}{10}\begin{bmatrix} 9/\sqrt{2} & -3 \\ 9 & -3/\sqrt{2} \end{bmatrix} z^{-2} + \frac{1}{10}\begin{bmatrix} -1/\sqrt{2} & 0 \\ -1 & 0 \end{bmatrix} z^{-3}.$$

One verifies that

$$\det H_0^G(z) = -\frac{1}{10} z^{-3}(1+z)^3$$

and the eigenvalues of $\frac{1}{2}H_0^G(1)$ are $\lambda_1 = 1$ and $\lambda_2 = -0.2$.

Since $|\lambda_2| < 1$, it follows from Proposition 4.2 that the cascade algorithm will produce the G-H-M multiscaling function and D-G-H-M multiwavelet, shown in Fig. 4.1, from any initial two-vector satisfying Remark 4.2.

### Strang–Strela piecewise linear multiscaling function

Strang and Strela [37] have produced a pair of orthonormal piecewise linear multiscaling function and multiwavelet, satisfying the orthogonality condition (4.31), with the following filters:

$$H_0^G(z) = \begin{bmatrix} 1 & 0 \\ \sqrt{3}/2 & 0 \end{bmatrix} + \begin{bmatrix} 1 & 0 \\ -\sqrt{3}/2 & 1/2 \end{bmatrix} z^{-1} + \begin{bmatrix} 0 & 0 \\ 0 & 1/2 \end{bmatrix} z^{-2}$$

$$H_1^G(z) = \frac{1}{\sqrt{7}}\begin{bmatrix} -1 & 0 \\ \sqrt{3}/2 & 0 \end{bmatrix} + \frac{1}{\sqrt{7}}\begin{bmatrix} 1 & 2\sqrt{3} \\ -\sqrt{3}/2 & 1/2 \end{bmatrix} z^{-1} + \frac{1}{\sqrt{7}}\begin{bmatrix} 0 & 0 \\ 0 & -7/2 \end{bmatrix} z^{-2}.$$

The product filter,

$$P(z) = H_0(z)H_0^T(z^{-1}),$$

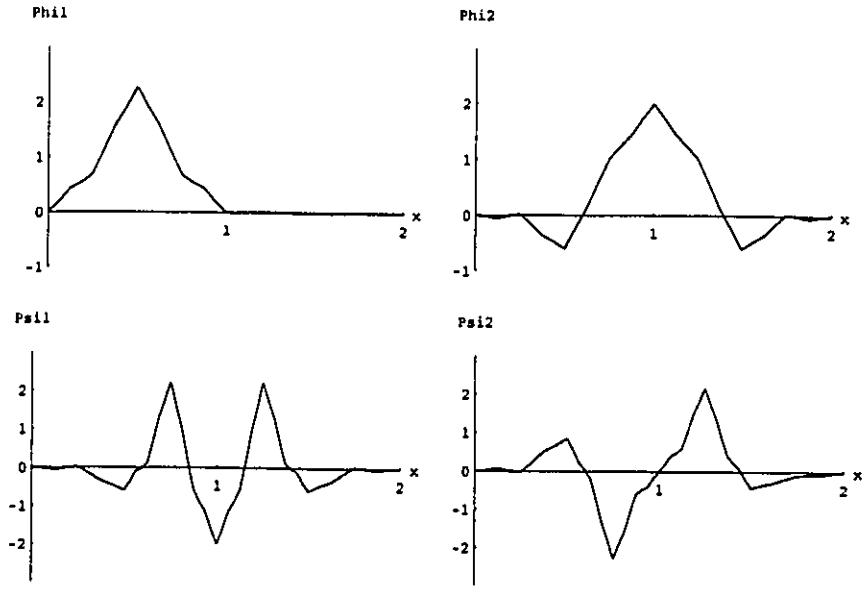


Figure 4.1: G-H-M multiscaling function and D-G-H-M multiwavelet.

has determinant

$$\det P(z) = \frac{1}{4} z^{-2}(1+z)^4.$$

The determinant of $H_0(z)$ is

$$\det H_0(z) = \frac{1}{2} z^{-3}(1+z)^2.$$

The eigenvalues of $\frac{1}{2}H_0(1)$ are $\lambda_1 = 1$ and $\lambda_2 = 0.5$. Since $|\lambda_2| < 1$, it follows from Proposition 4.2 that the cascade algorithm will converge to the Strang–Strela multiscaling function and multiwavelet, shown in Fig. 4.2, from any two-vector values satisfying Remark 4.2

### Cooklev's nonsymmetric multiwavelets

As an example of multiscaling function whose product filter,

$$P(z) = H_0(z)H_0^T(z^{-1}) = \begin{bmatrix} p^{11}(z) & p^{12}(z) \\ p^{21}(z) & p^{P22}(z) \end{bmatrix},$$

satisfies

$$P(z) + P(-z) = I$$

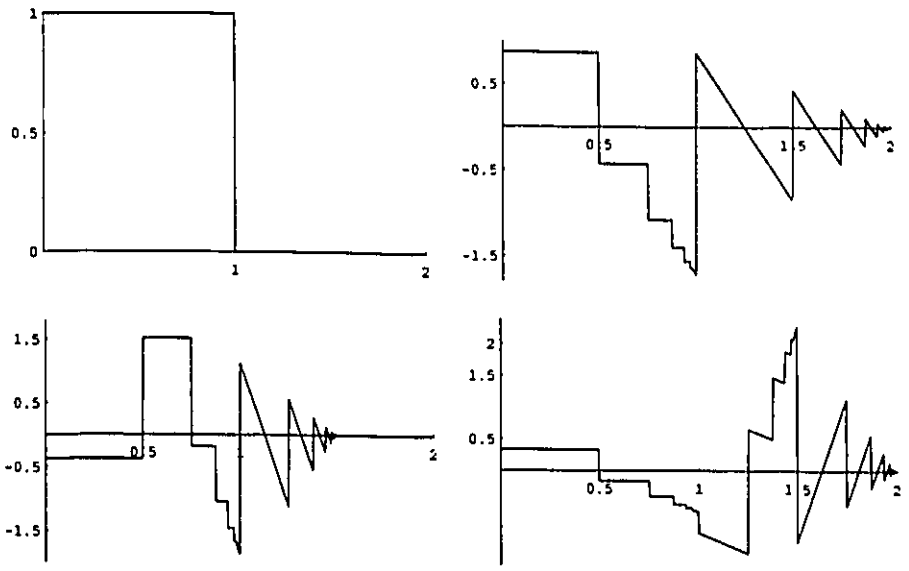

Figure 4.2: Strang–Strela's piecewise linear multiscaling function and multiwavelet.

and

$$\det P(z) = z^4(1+z^{-1})^8,$$

is given in [5], pp. 196–199. Here $P(z)$ is given to a precision of $10^{-3}$:

$$\begin{aligned}
p^{11}(z) &= 63.71922217 + 24.24699963(z^{-1}+z) + 8.03533024(z^{-3}+z^3),\\
p^{12}(z) &= 1.73714280357z^{-1} - 3.413316119z + 1.73714280357z^3,\\
p^{21}(z) &= 1.73714280357z^{-3} - 3.413316119z^{-1} + 1.73714280357z,\\
p^{22}(z) &= 0.9956031378 + 0.5(z^{-1}+z).
\end{aligned}$$

By spectral factorization, $H_0(z)$ is found, to a precision of $10^{-3}$ to be

$$\begin{aligned}
h_0^{(0)} &= \begin{bmatrix} 1.75167877900545 & 0.0 \\ 2.37892314369563 & 0.685375014813871 \end{bmatrix},\\
h_1^{(0)} &= \begin{bmatrix} 4.544528207816465 & 0.000975993758244328 \\ -2.25450962889358 & 0.7251643084881315 \end{bmatrix},\\
h_2^{(0)} &= \begin{bmatrix} 3.890440724620659 & 0.0 \\ -2.582798346116616 & 0.0 \end{bmatrix},\\
h_3^{(0)} &= \begin{bmatrix} 1.110456699381924 & 0.0 \\ 2.493296531394941 & 0.0 \end{bmatrix}.
\end{aligned}$$

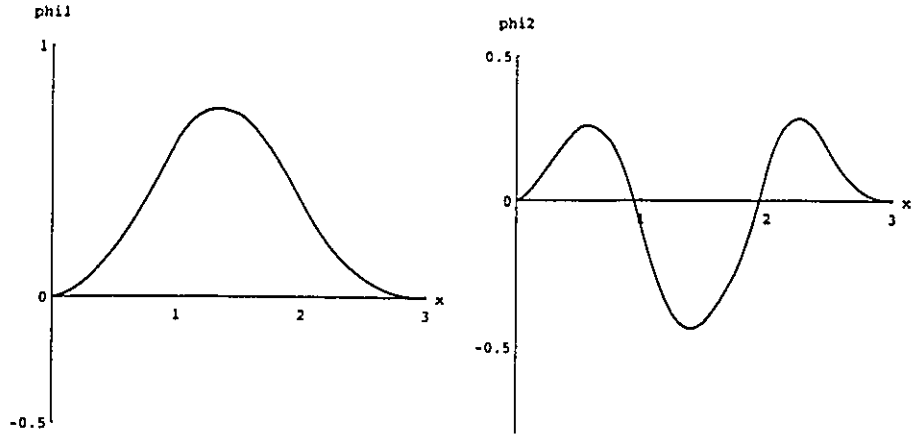


Figure 4.3: Cooklev's nonsymmetric multiscaling function.

The corresponding scaling functions (see Fig. 4.3) are nonsymmetric because of the lower triangular $h_0^{(0)}$.

The eigenvalues of $\frac{1}{2}H_0(1)$ are $\lambda_1 \approx 0.9985$ and $\lambda_2 \approx 0.1247$. Since $\lambda_1 \approx 1$ and $|\lambda_2| < 1$, it follows from Proposition 4.2 that the cascade algorithm will converge to the two scaling functions shown in Fig. 4.3 from any two-vector values satisfying Remark 4.2. It seems that the multiscaling function does not have vanishing moments of order at least one since $H_0(z)$ does not satisfies the basic condition 1.6 given in [34]. Moreover, the orthogonality condition

$$H_0(\omega/2)H_0^*(\omega/2) + H_0(\omega/2+\pi)H_0^*(\omega/2+\pi) = I$$

is not satisfied by the multiscaling function.

### Ashino–Nagase–Vaillancourt simple multiwavelets

The multiwavelets of D-G-H-M and Strang–Strela have good time localization at the expense of frequency localization. To achieve better frequency resolution, I. Daubechies in [11] suggested split-type orthonormal wavelets generated by the tensor product of two one-dimensional wavelet bases. In [1], R. Ashino, M. Nagase and R. Vaillancourt extended this to split-type multiwavelets.

As in Chapter 2, let $m_0$ and $m_1$ be defined by

$$m_0(\xi) = \frac{1}{\sqrt{2}} \sum_n h_n e^{-in\xi},$$
$$m_1(\xi) = -e^{-i\xi}\overline{m_0(\xi+\pi)}.$$

Multifilters for this type of multiwavelets are constructed in the form

$$M_0(\xi) = \begin{bmatrix} m_0(\xi) & 0 \\ m_1(\xi) & 0 \end{bmatrix}, \qquad M_1(\xi) = \begin{bmatrix} 0 & \widetilde{m}_0(\xi) \\ 0 & \widetilde{m}_1(\xi) \end{bmatrix}$$

where $m_0$, $m_1$, $\widetilde{m}_0$, $\widetilde{m}_1 \in C^\infty$ satisfy the orthogonality relations

$$|m_0(\xi)|^2 + |m_0(\xi+\pi)|^2 = 1,$$
$$|m_1(\xi)|^2 + |m_1(\xi+\pi)|^2 = 1,$$
$$m_0(\xi)\overline{m_1(\xi)} + m_0(\xi+\pi)\overline{m_1(\xi+\pi)} = 0,$$

$$|\widetilde{m}_0(\xi)|^2 + |\widetilde{m}_0(\xi+\pi)|^2 = 1,$$
$$|\widetilde{m}_1(\xi)|^2 + |\widetilde{m}_1(\xi+\pi)|^2 = 1,$$
$$\widetilde{m}_0(\xi)\overline{\widetilde{m}_1(\xi)} + \widetilde{m}_0(\xi+\pi)\overline{\widetilde{m}_1(\xi+\pi)} = 0.$$

Therefore, the block matrix

$$\begin{bmatrix} M_0(\xi) & M_0(\xi+\pi) \\ M_1(\xi) & M_1(\xi+\pi) \end{bmatrix}$$

is a $4 \times 4$ unitary matrix, and the corresponding multiwavelet is

$$\widehat{\Psi}(\xi) = \begin{bmatrix} \widehat{\psi}_1(\xi) \\ \widehat{\psi}_2(\xi) \end{bmatrix} = M_1(\xi/2) \begin{bmatrix} \widehat{\phi}(\xi/2) \\ \widehat{\psi}(\xi/2) \end{bmatrix} = \begin{bmatrix} \widetilde{m}_0(\xi/2)\widehat{\psi}(\xi/2) \\ \widetilde{m}_1(\xi/2)\widehat{\psi}(\xi/2) \end{bmatrix}$$

with the multiscaling function

$$\widehat{\Phi}(\xi) = \begin{bmatrix} \widehat{\phi}_1(\xi) \\ \widehat{\phi}_2(\xi) \end{bmatrix} = M_0(\xi/2) \begin{bmatrix} \widehat{\phi}(\xi/2) \\ \widehat{\psi}(\xi/2) \end{bmatrix} = \begin{bmatrix} m_0(\xi/2)\widehat{\phi}(\xi/2) \\ m_1(\xi/2)\widehat{\phi}(\xi/2) \end{bmatrix}.$$

This method produces perhaps the simplest multiwavelets, but these multiwavelets cannot achieve symmetry and orthogonality at the same time if the support is compact.

The support of these multiwavelets is shorter than the support of the individual wavelets used to build the multiwavelets.

### Cooklev's real multiwavelets from complex wavelets

Using the $z$-notation, Cooklev has represented Lawton's complex wavelets (described in the previous and the next chapters) as multiwavelets or filterbanks in the form

$$H_0(z) = \begin{bmatrix} H_0^R(z) & -H_0^I(z) \\ H_0^I(z) & H_0^R(z) \end{bmatrix},$$
$$H_1(z) = \begin{bmatrix} H_1^R(z) & -H_1^I(z) \\ H_1^I(z) & H_1^R(z) \end{bmatrix},$$

where $H_i^R$ and $H_i^I$, $i = 1, 2$, denote the real and imaginary parts of $H_i$, respectively.

To construct an orthogonal perfect reconstruction multifilter pair, $H_0(z)$ and $H_1(z)$ are forced to satisfy conditions (4.3)-(4.6). Since $H_i^R$ and $H_i^I$ comes from a complex-valued scalar filter, the symmetry of $H_0$ and $H_1$ is connected with the symmetry of the polynomials $H_i^R(z)$ and $H_i^I(z)$, $i = 1, 2$.

This method to get $H_0$ and $H_1$ by representing a complex number by a matrix,

$$z = x + iy \Leftrightarrow \begin{bmatrix} x & y \\ -y & x \end{bmatrix},$$

offers a straightforward way to construct multiwavelets from complex wavelets. We remark that these multiscaling functions and multiwavelets, considered as real two-vector functions, do not satisfy the orthogonality condition (4.31).

Figures for Cooklev's multiwavelets are found in the next chapter.

## 4.3 Summary

In the previous two sections, we studied the basic multiwavelet theory and three types of multiwavelets. There are other methods of construction of multiwavelets which we did not mention such as the construction with separable multifilters, etc. Also, there are some general properties of multiwavelets such as the method to calculate the regularity of multiwavelets, which have not been described here.

It is worth mentioning the general method for designing multifilters. In section 4.1, we discussed it according to Proposition 4.1. It did open our eyes to the idea, but there is still considerable freedom in the design of the product filter. The product multifilter from G-H-M has determinant $z^3(1 + z^{-1})^6$, the product multifilter from

Strang and Strela, has determinant $z^2(1+z^{-1})^4$ and the product multifilter of Cooklev has determinant $z^4(1+z^{-1})^8$. These determinants have multiple zeros at $z=-1$. If, at $z=1$, the low pass matrix filter has the simple eigenvalue 1 and the remaining eigenvalues lie inside the unit disk, then, by results of A. Cohen, I. Daubechies and G. Plonka [4] and C. Heil and D. Colella [18], the cascade algorithm produces unique multiscaling functions and multiwavelets from any starting values satisfying the conditions of Remark 4.2.

Corresponding to the examples described in Section 4.2, we see that there are always some properties which cannot be considered with other properties in every method. Therefore, the question arises: can we find an approach to construct multiwavelets with orthogonality, symmetry, flexible support length and arbitrarily high number of vanishing moments? This question has been addressed by Strela [38] and Plonka and Strela [33].

# Chapter 5

# Numerical Results

In this chapter, we give some examples obtained by using the techniques described in the previous chapters.

The integer $N$ will stand for the number of vanishing moments of the corresponding wavelets. Seven interations of the constructive cascade algorithm are used to produce the scaling functions and the corresponding wavelets.

In Tables 5.1–5.7, we list the filter coefficients ${}_N h_n$ for Lawton's compactly supported complex-valued scalar wavelets. The ${}_N h_n$ are normalized so that $\sum_n {}_N h_n = \sqrt{2}$.

## 5.1 Lawton's complex filters

In this section we list the coefficients of Lawton's complex filters for $N = 3, \ldots, 8$. These coefficients have been obtained in double precision by spectral factorization and appropriate choices of the zeros of the corresponding polynomials as described in Chapter 3. Figures are drawn for Lawton's filters and some of the corresponding Daubechies real filters.

Table 5.1: Real and imaginary parts of coefficients of Lawton's complex filters ($N$=3, 4).

| $N$ | Real part | Imaginary part |
|---|---|---|
| 3 | 1.0 | 0.0 |
| | 0.0 | 1.290994448735805 |
| | −5.0 | 3.872983346207415 |
| | −5.0 | 3.872983346207415 |
| | 0.0 | 1.290994448735805 |
| | 1.0 | 0.0 |
| 4 | −0.3288759177860308 | 0.0 |
| | 0.4459203153501978 | −0.4919071368212055 |
| | 2.428332711191807 | −0.4719059655503813 |
| | −0.3233906644553652 | 3.031447506010529 |
| | −5.1478263402245 | 7.00670694312182 |
| | −2.815006925782846 | 5.490983190116556 |
| | 1.355892271930708 | 1.49572258173444 |
| | 1.0 | 0.0 |

## 5.2 Figures of filters and multifilters

In Figs. 5.1–5.22, we present four sets of graghs of scaling functions and wavelets, namely Daubechies' real-valued scaling functions and wavelets, Lawton's complex-valued scaling functions and wavelets and Cooklev's multiscaling functions and multiwavelets, corresponding to $N = 3$, 5, 7 and 9. These scaling functions and wavelets are symmetric or antisymmetric. In Figs. 5.23–5.30 we present Daubechies' wavelets, Lawton's wavelets and Cooklev's multiscaling functions and multiwavelets corresponding to $N = 4$ and 6. These scaling functions and wavelets are nonsymmetric. It should be noted that we have presented all the possible choices of the different pairs of roots. For $N = 9$, there are 8 different pairs of roots, but here we present the figures for only two of them.

Table 5.2: Real and imaginary parts of coefficients of Lawton's complex filters ($N$=5a, 5b).

| $N$ | Real part | Imaginary part |
|---|---|---|
| 5a | 1.0 | 0.0 |
| | 0.0 | 0.831886572169963 |
| | −6.13173192019257 | 0.7917661169179349 |
| | −0.6586596009630741 | −7.687581425789803 |
| | 19.68268079807375 | −21.19836885676934 |
| | 19.68268079807376 | −21.19836885676934 |
| | −0.6586596009630626 | −7.687581425789798 |
| | −6.131731920192565 | 0.7917661169179358 |
| | 0.0 | 0.831886572169963 |
| | 1.0 | 0.0 |
| 5b | 1.0 | 0.0 |
| | 0.0 | 2.146102088992586 |
| | −8.08859137390339 | 4.866011231748732 |
| | −10.44295686951719 | −5.715373087152539 |
| | 0.1140862609655073 | −26.45346079725317 |
| | 0.1140862609655073 | −26.45346079725317 |
| | −10.44295686951719 | −5.715373087152539 |
| | −8.08859137390339 | 4.866011231748732 |
| | 0.0 | 2.146102088992586 |
| | 1.0 | 0.0 |

Table 5.3: Real and imaginary parts of coefficients of Lawton's complex filters ($N$=6a, 6b).

| $N$ | Real part | Imaginary part |
|---|---|---|
| 6a | −0.3525429847631032 | 0.0 |
| | 0.4378567219471435 | −0.1612263943365642 |
| | 2.833009948217348 | 0.3338646425068745 |
| | −2.466420032719199 | 2.8339681132780? |
| | −10.10934132288158 | 1.421297178983743 |
| | 6.776550724343143 | −11.97460163814514 |
| | 31.09144971014476 | −25.6886325726374 |
| | 21.30160056972714 | −21.53201718949971 |
| | −1.730092397784233 | −7.168760006351443 |
| | −4.075109753558128 | 0.1889704260123404 |
| | 1.241995276806895 | 0.4573240748072259 |
| | 1.0 | 0.0 |
| 6b | −0.3525429847631032 | 0.0 |
| | 0.4378567219471439 | −0.849383278203893 |
| | 3.81935492332577 | −0.7232582508071488 |
| | 0.6538492156268676 | 7.077909452588108 |
| | −12.10097031008202 | 12.4997205586225 |
| | −15.46355880805532 | −7.117944144125023 |
| | −10.06938770931809 | −31.75291375656898 |
| | −14.74733861418923 | −22.71889992923275 |
| | −17.53055103650256 | 1.995064442738126 |
| | −6.872910355862587 | 8.03623504851984 |
| | 1.241995276806895 | 2.409304155561767 |
| | 1.0 | 0.0 |

Table 5.4: Real and imaginary parts of coefficients of Lawton's complex filters ($N$=7a, 7b).

| $N$ | Real part | Imaginary part |
|---|---|---|
| 7a | 1.0 | 0.0 |
| | $1.438849039914203 \times 10^{-13}$ | 2.9305252116394 |
| | −11.97580718984453 | 6.110930406015826 |
| | −17.90823562140083 | −17.0745931076402 |
| | 15.98914477600771 | −58.86683141967491 |
| | 62.38680688430644 | −33.14082805110399 |
| | 76.63931213167729 | 52.62692486547231 |
| | 76.63931213167726 | 52.62692486547229 |
| | 62.38680688430646 | −33.14082805110396 |
| | 15.98914477600778 | −58.86683141967487 |
| | −17.90823562140083 | −17.07459310764019 |
| | −11.97580718984453 | 6.110930406015829 |
| | $1.447730824111204 \times 10^{-13}$ | 2.9305252116394 |
| | 1.0 | 0.0 |
| 7b | 1.0 | 0.0 |
| | $1.438849039914203 \times 10^{-13}$ | 0.1936998107325399 |
| | −7.700577990156376 | 2.18242267614775 |
| | −0.4227348593065159 | 6.948569279606624 |
| | 22.95646171908758 | 4.629458127662693 |
| | −19.31674307896992 | −19.31348858203644 |
| | −119.3864799360843 | −49.95887759444824 |
| | −119.3864799360843 | −49.95887759444822 |
| | −19.31674307896998 | −19.31348858203638 |
| | 22.95646171908754 | 4.629458127662728 |
| | −0.4227348593065159 | 6.948569279606633 |
| | −7.700577990156372 | 2.182422676147751 |
| | $1.447730824111204 \times 10^{-13}$ | 0.1936998107325399 |
| | 1.0 | 0.0 |

Table 5.5: Real and imaginary parts of coefficients of Lawton's complex filters ($N$=7c, 7d).

| $N$ | Real part | Imaginary part |
|---|---|---|
| 7c | 1.0 | 0.0 |
| | $1.447730824111204 \times 10^{-13}$ | −2.071825245627513 |
| | −9.82804810602721 | −3.478153151665104 |
| | −7.206125507776627 | 14.92651298687195 |
| | 32.91442030830939 | 38.86518208974296 |
| | 61.61641546959584 | −5.039477407932414 |
| | 45.28669926705027 | −96.4454511013251 |
| | 45.28669926705024 | −96.4454511013251 |
| | 61.61641546959578 | −5.039477407932381 |
| | 32.91442030830936 | 38.86518208974297 |
| | −7.206125507776648 | 14.92651298687196 |
| | −9.82804810602721 | −3.478153151665101 |
| | $1.447730824111204 \times 10^{-13}$ | −2.071825245627513 |
| | 1.0 | 0.0 |
| 7d | 1.0 | 0.0 |
| | $1.438849039914203 \times 10^{-13}$ | −0.6650001552793477 |
| | −7.902930785078248 | −0.4503545782029717 |
| | −0.2994858644340397 | 6.434530727108367 |
| | 29.28273014608556 | 5.99627674472907 |
| | 4.5185292801489 | −37.03767526159686 |
| | −76.82808687531349 | −99.3145049229234 |
| | −76.82808687531352 | −99.3145049229234 |
| | 4.518529280148926 | −37.03767526159689 |
| | 29.28273014608558 | 5.996276744729059 |
| | −0.2994858644340184 | 6.434530727108364 |
| | −7.902930785078241 | −0.4503545782029717 |
| | $1.447730824111204 \times 10^{-13}$ | −0.665000155279347 |
| | 1.0 | 0.0 |

Table 5.6: Real and imaginary parts of coefficients of Lawton's complex filters ($N$=8a, 8b).

| $N$ | Real part | Imaginary part |
|---|---|---|
| 8a | −0.3654035130767648 | 0.0 |
| | 0.4332401363153551 | −1.175671899258328 |
| | 5.468628318386223 | −0.966936924202706 |
| | 2.154412990202434 | 12.82761730601287 |
| | −25.39526029108023 | 22.02190553865803 |
| | −41.62756038658029 | −29.14360359356 |
| | −1.564633930407763 | −95.4488486955918 |
| | 62.33627814247862 | −53.26717138311495 |
| | 100.5263446742042 | 29.39063303150425 |
| | 99.640680378049 | −7.650386189351594 |
| | 50.05527753116172 | −87.5951515487718 |
| | −14.0576688028018 | −69.1980613464433 |
| | −31.31921193253186 | −7.950565603455275 |
| | −11.28799307598986 | 10.27577485259034 |
| | 1.185648525017842 | 3.217461948734303 |
| | 1.0 | 0.0 |
| 8b | −0.3654035130767648 | 0.0 |
| | 0.4332401363153547 | −0.221637056148777 |
| | 3.644505968244319 | −0.864625659408783 |
| | −2.594995370261593 | 0.109083378809105 |
| | −12.82333067360978 | 6.051100091854874 |
| | 16.02397217567745 | 12.81905629460162 |
| | 39.0895326298611 | 8.19932589856566 |
| | −56.65414987944823 | −10.21125730200725 |
| | −176.8374106092276 | −26.00877486465673 |
| | −135.5546135069382 | −22.71101749657261 |
| | −16.29781508577406 | −4.783487884606011 |
| | 14.75438336534211 | 8.86005978526359 |
| | −6.48380673392083 | 9.24873761362526 |
| | −6.295916413172762 | 3.804541847797286 |
| | 1.185648525017842 | 0.60655425636867 |
| | 1.0 | 0.0 |

Table 5.7: Real and imaginary parts of coefficients of Lawton's complex filters ($N$=8c, 8d).

| $N$ | Real part | Imaginary part |
|---|---|---|
| 8c | −0.3654035130767648 | 0.0 |
| | 0.4332401363153547 | 0.6613053412153862 |
| | 4.175701969061297 | 0.0916167965306238 |
| | −2.323818396514227 | −8.05263946951064 |
| | −22.33651830171234 | −7.478584027994018 |
| | −7.554104200569189 | 32.76567068736411 |
| | 50.1862328116619 | 56.74814685320867 |
| | 70.5665170579438 | −27.87749101355935 |
| | 54.66929627531263 | −131.4449547500384 |
| | 72.20464419690774 | −96.6439114761984 |
| | 79.33035967470545 | 9.46143090484678 |
| | 29.59533017556049 | 38.95561165539702 |
| | −10.6731492790571 | 9.69839607664202 |
| | −7.749640807731013 | −4.542288571204864 |
| | 1.185648525017842 | −1.809794699692604 |
| | 1.0 | 0.0 |
| 8d | −0.3654035130767648 | 0.0 |
| | 0.4332401363153551 | 0.2927295018941654 |
| | 3.694543222009351 | 0.01069446826330411 |
| | −3.051543670543708 | −3.043360107515777 |
| | −16.25684463452721 | 0.04766271281203771 |
| | 10.859132769742 | 19.10482564738217 |
| | 50.07923019909295 | 13.43101259654665 |
| | −4.533581947011819 | −64.15106790158599 |
| | −89.673282535801 | −143.9198764220257 |
| | −55.59964106164756 | −121.6476355347244 |
| | 25.79496076632876 | −38.00043119359607 |
| | 26.22501019443524 | 5.201918468106044 |
| | −5.559089001482733 | 3.060516470640859 |
| | −6.43285339372806 | −1.928944433588192 |
| | 1.185648525017842 | −0.801112992673029 |
| | 1.0 | 0.0 |

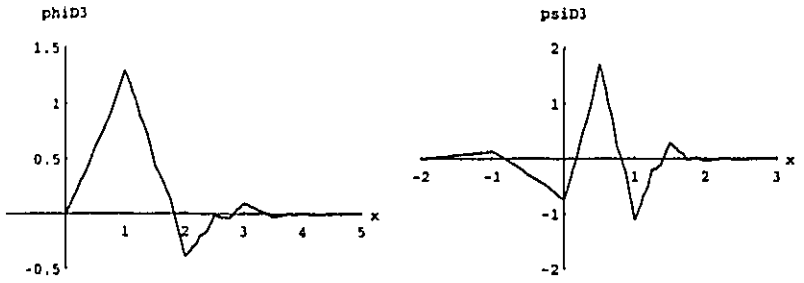


Figure 5.1: Real scaling function and wavelet D3.

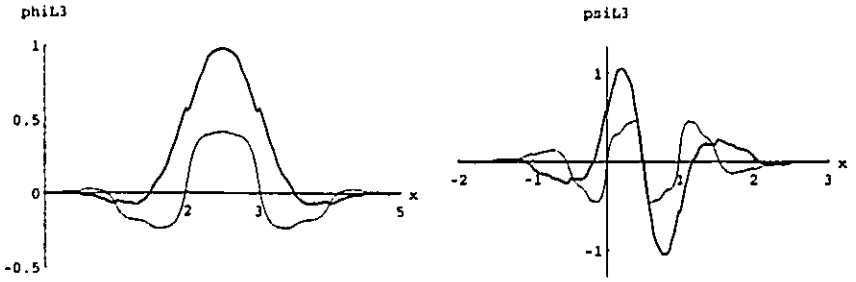


Figure 5.2: Real (bold lines) and imaginary parts of complex scaling function and wavelet L3 with starting value $\delta_{n0}$.

### Symmetric and antisymmetric figures for $N = 3$

The following figures present Daubechies' real-valued scaling functions and wavelets, Lawton's complex-valued scaling functions and wavelets and Cooklev's multiscaling functions and multiwavelets for $N = 3$.

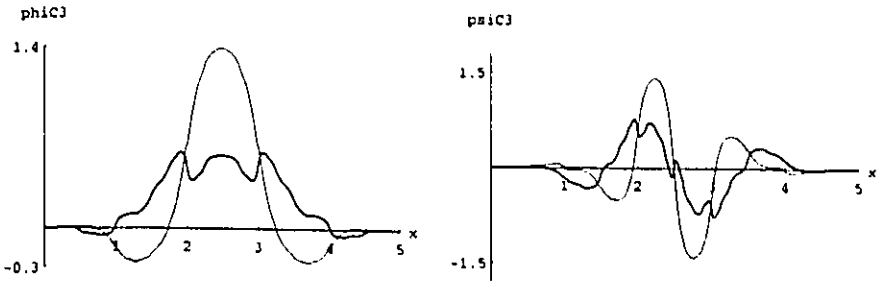


Figure 5.3: Real multiscaling functions and multiwavelets C3 with starting value $[1\ 1]^T\delta_{n0}$.

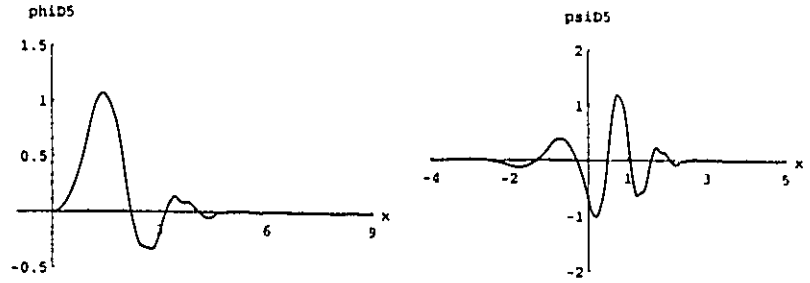


Figure 5.4: Real scaling function and wavelet D5

**Symmetric and antisymmetric figures for $N = 5$.**

In this subsection, we present Daubechies' real-valued scaling functions and wavelets, Lawton's complex-valued scaling functions and wavelets and Cooklev's multiscaling functions and multiwavelets corresponding to $N = 5$. In this case, there are two pairs of roots, referred to as $N = 5$a and $N = 5$b, corresponding to two sets of scaling functions and wavelets. For Daubechies' case, we only present one pair of roots.

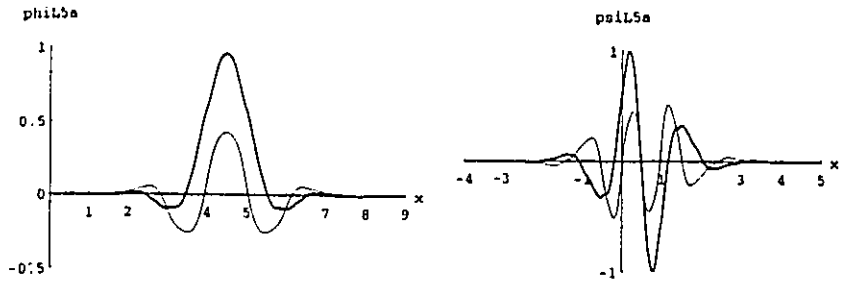


Figure 5.5: Real (bold lines) and imaginary parts of complex scaling function and wavelet L5a with starting value $\delta_{n0}$.

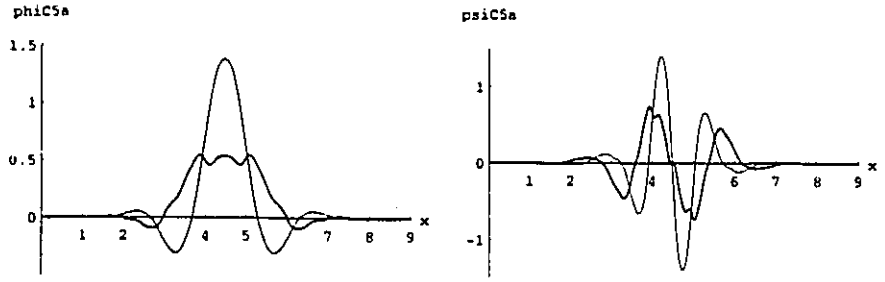


Figure 5.6: Real multiscaling functions and multiwavelets C5a with starting value $[1\ 1]^T\delta_{n0}$.

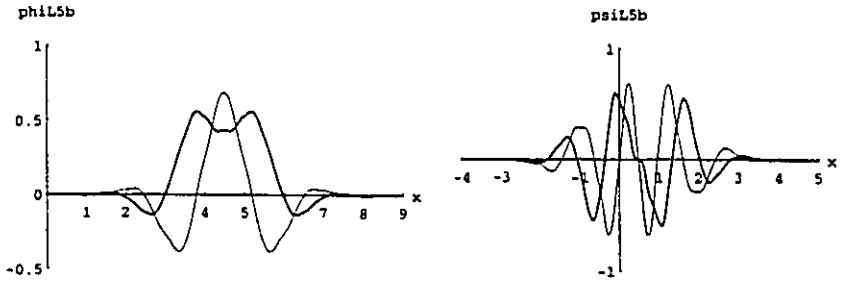


Figure 5.7: Real (bold lines) and imaginary parts of complex scaling function and wavelet L5b with starting value $\delta_{n0}$.

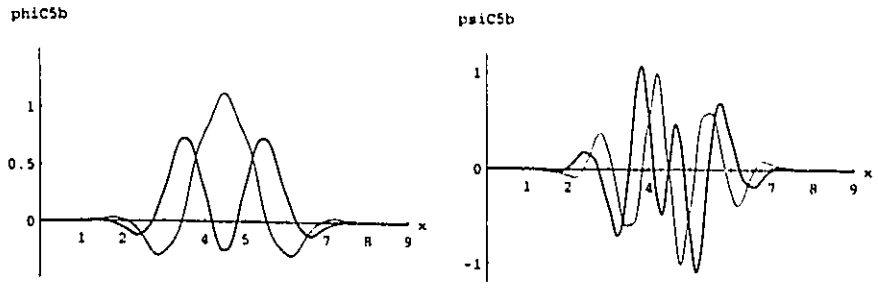


Figure 5.8: Real multiscaling functions and multiwavelets C5b with starting value $[1\ 1]^T\delta_{n0}$.

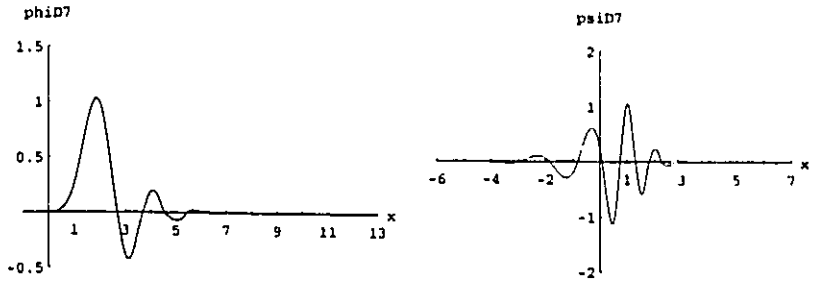


Figure 5.9: Real scaling function and wavelet D7.

### Symmetric and antisymmetric figures for $N = 7$

In this subsection, we plot Daubechies' real-valued scaling functions and wavelets, Lawton's complex-valued scaling functions and wavelets and Cooklev's multiscaling functions and multiwavelets corresponding to $N = 7$. In this case, there are four pairs of roots, identified as $N = 7$a, $N = 7$b, $N = 7$c and $N = 7$d, corresponding to four sets of scaling functions and wavelets. For Daubechies' case, we only present one pair of roots.

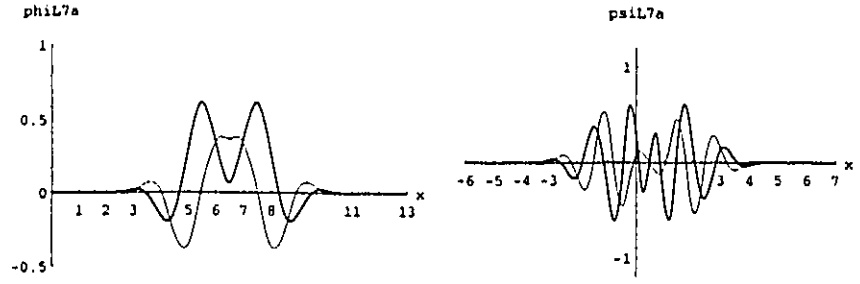


Figure 5.10: Real (bold lines) and imaginary parts of complex scaling function and wavelet L7a with starting value $\delta_{n0}$.

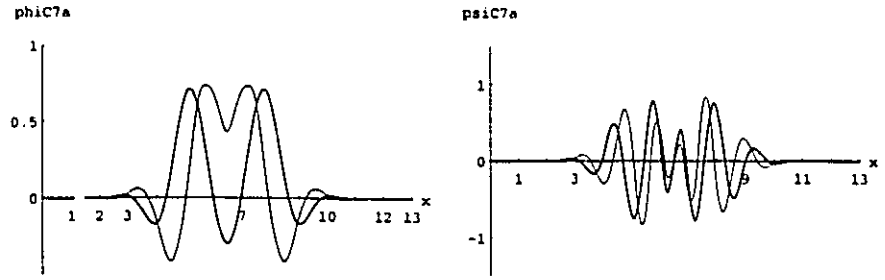


Figure 5.11: Real multiscaling functions and multiwavelets C7a with starting value $[1\ 1]^T\delta_{n0}$.

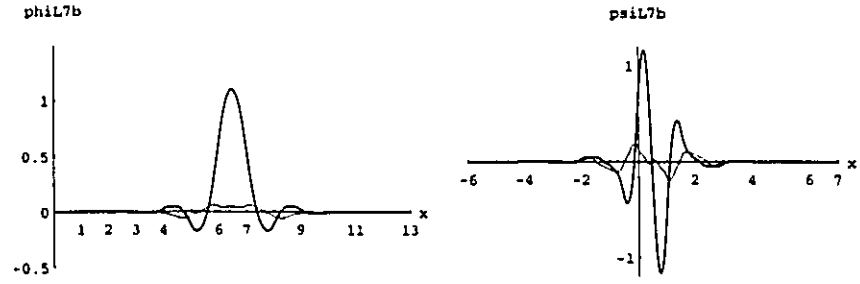


Figure 5.12: Real (bold lines) and imaginary parts of complex scaling function and wavelet L7b with starting value $\delta_{n0}$.

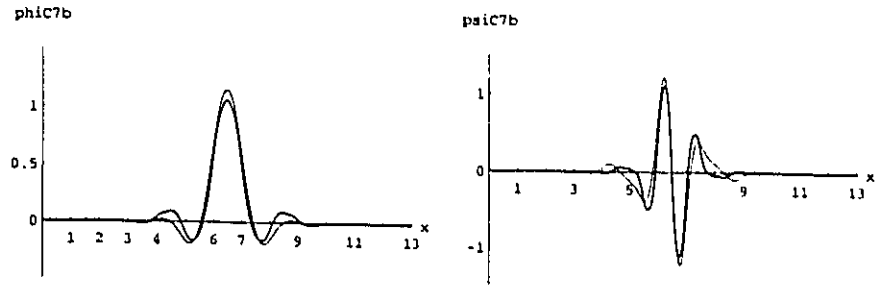


Figure 5.13: Real multiscaling functions and multiwavelets C7b with starting value $[1\ 1]^T\delta_{n0}$.

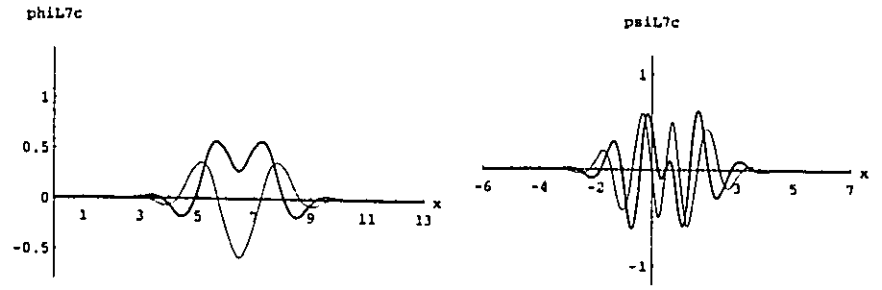


Figure 5.14: Real (bold lines) and imaginary parts of complex scaling function and wavelet L7c with starting value $\delta_{n0}$.

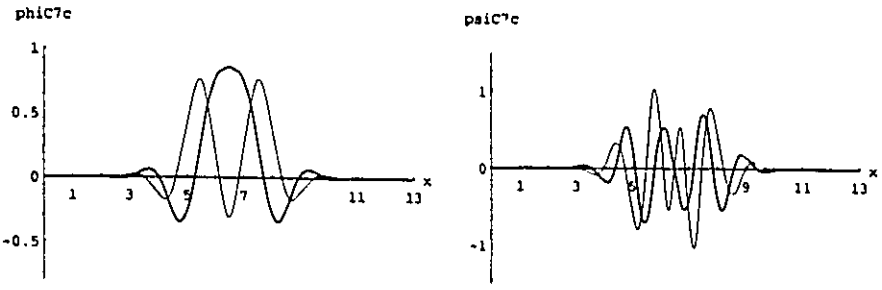


Figure 5.15: Real multiscaling functions and multiwavelets C7c with starting value $[1\ 1]^T\delta_{n0}$.

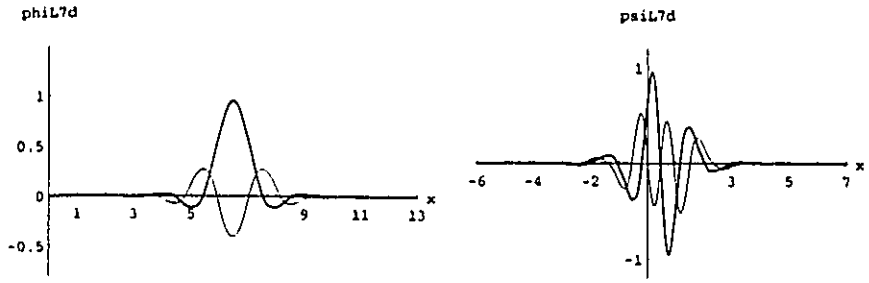


Figure 5.16: Real (bold lines) and imaginary parts of complex scaling function and wavelet L7d with starting value $\delta_{n0}$.

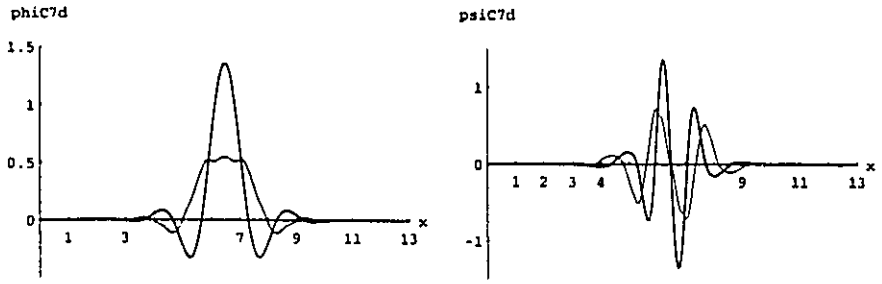


Figure 5.17: Real multiscaling functions and multiwavelets C7d with starting value $[1\ 1]^T\delta_{n0}$.

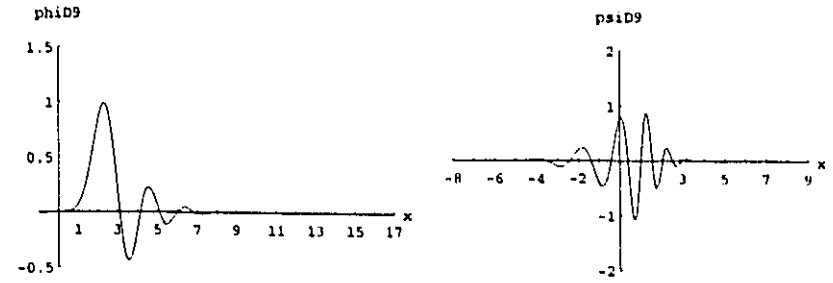


Figure 5.18: Real scaling function and wavelet D9.

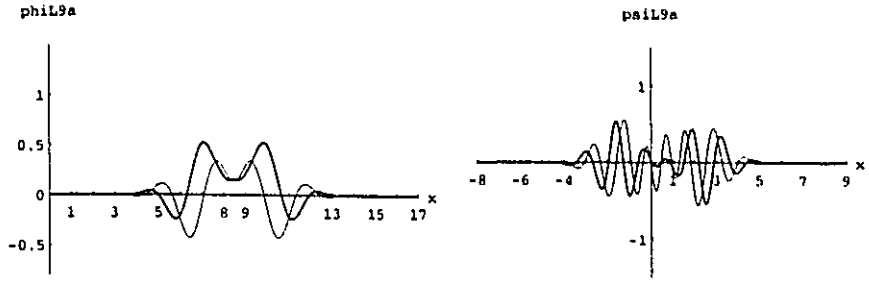


Figure 5.19: Real (bold lines) and imaginary parts of complex scaling function and wavelet L9a with starting value $\delta_{n0}$.

### Symmetric and antisymmetric figures for $N = 9$

The following are Daubechies' real-valued scaling functions and wavelets, Lawton's complex-valued scaling functions and wavelets and Cooklev's multiscaling functions and multiwavelets corresponding to $N = 9$. In this case, there are eight pairs of roots corresponding to eight sets of scaling functions and wavelets. Here, we only give two cases. For Daubechies' case, we only present one pair of roots.

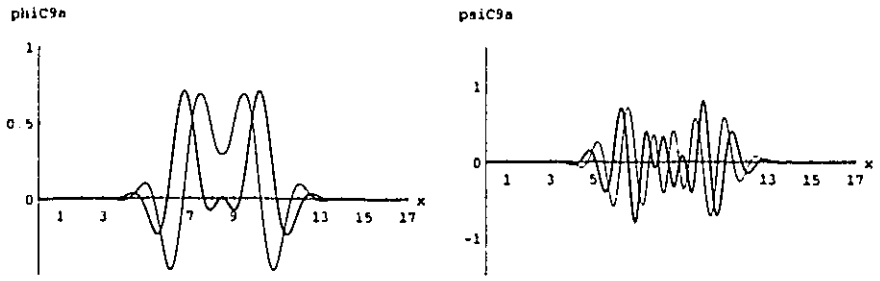


Figure 5.20: Real multiscaling functions and multiwavelets C9a with starting value $[1\ 1]^T\delta_{n0}$.

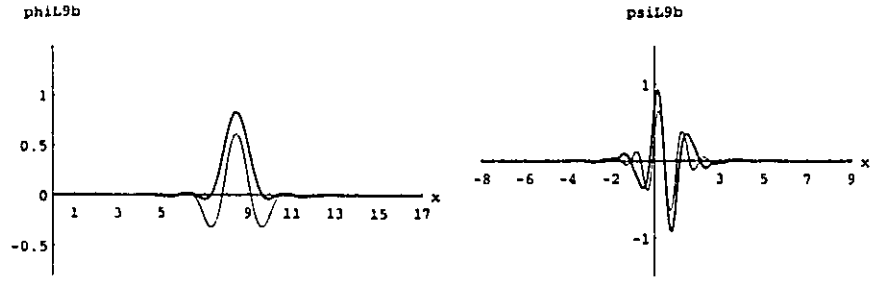


Figure 5.21: Real (bold lines) and imaginary parts of complex scaling function and wavelet L9b with starting value $\delta_{n0}$.

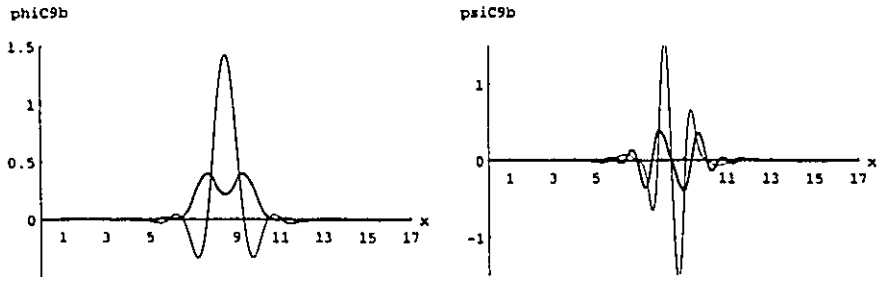


Figure 5.22: Real multiscaling functions and multiwavelets C9b with starting value $[1\ 1]^T\delta_{n0}$.

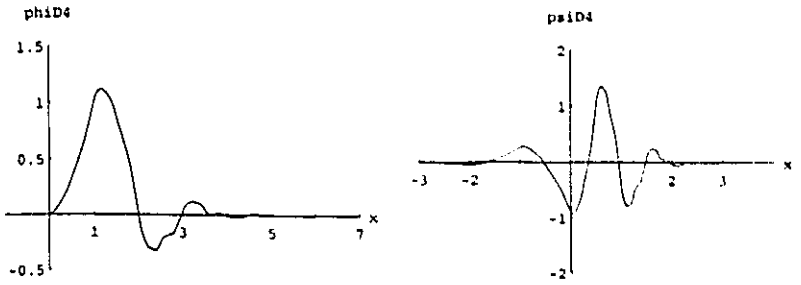


Figure 5.23: Real scaling function and wavelet D4.

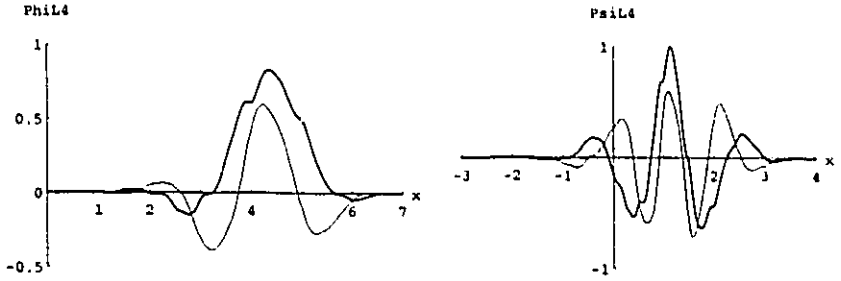


Figure 5.24: Real (bold lines) and imaginary parts of complex scaling function and wavelet L4 with starting value $\delta_{n0}$.

### Nonsymmetric figures for $N = 4$

In this subsection, we present Daubechies' real-valued scaling functions and wavelets, Lawton's complex-valued scaling functions and wavelets and Cooklev's multiscaling functions and multiwavelets corresponding to $N = 4$. For $N = 4$, the plots are asymmetric.

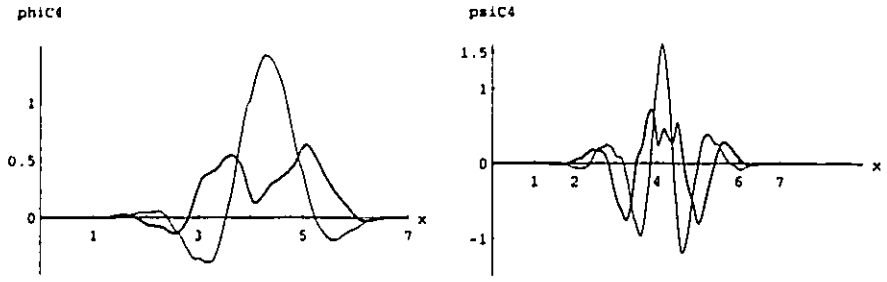


Figure 5.25: Real multiscaling functions and multiwavelets C4 with starting value $[1\ 1]^T\delta_{n0}$.

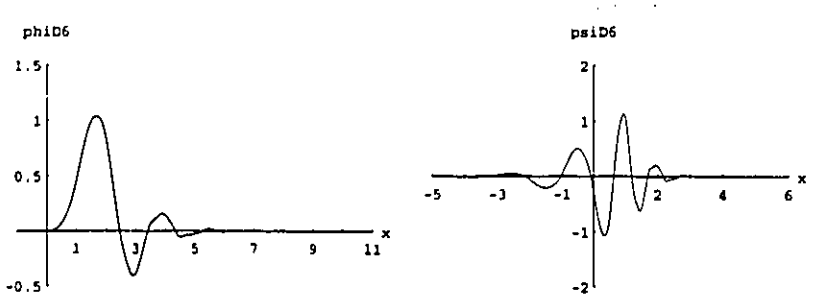


Figure 5.26: Real scaling function and wavelet D6.

**Nonsymmetric figures for $N = 6$**

The following are Daubechies' real-valued scaling functions and wavelets, Lawton's complex-valued scaling functions and wavelets and Cooklev's multiscaling functions and multiwavelets corresponding to $N = 6$. In this case, there are two pairs of roots, identified as $N = 6$a and $N = 6$b, corresponding to two sets of scaling functions and wavelets. For Daubechies' case, we only present one pair of roots. Since $N = 6$, the plots are asymmetric.

## 5.3 Comparison of multifilters

The most obvious property one sees in the above graphs is either symmetry/antisymmetry or asymmetry. Daubechies' scaling functions and wavelets are asymmetric. Lawton's complex-valued scaling functions and wavelets as well as Cooklev's multiscaling functions and multiwavelets are symmetric or antisymmetric only when $N$ is odd, for the reasons explained in Chapters 2 and 3. Another visible property is the support length

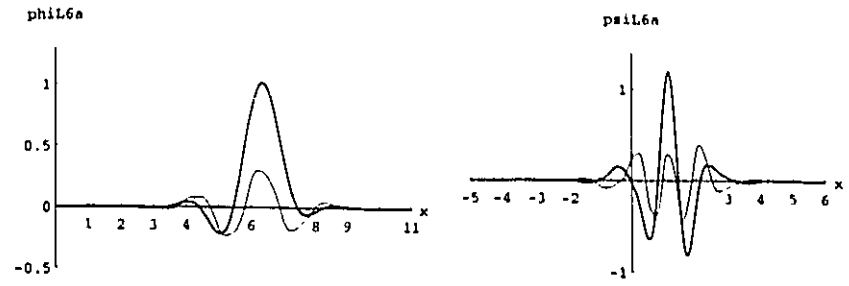


Figure 5.27: Real (bold lines) and imaginary parts of complex scaling function and wavelet L6a with starting value $\delta_{n0}$.

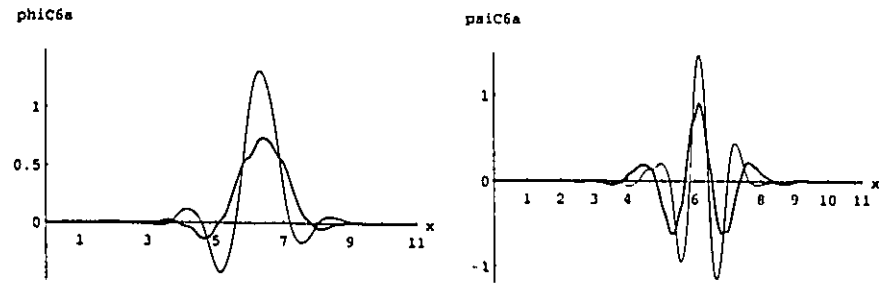


Figure 5.28: Real multiscaling functions and multiwavelets C6a with starting value $[1\ 1]^T\delta_{n0}$.

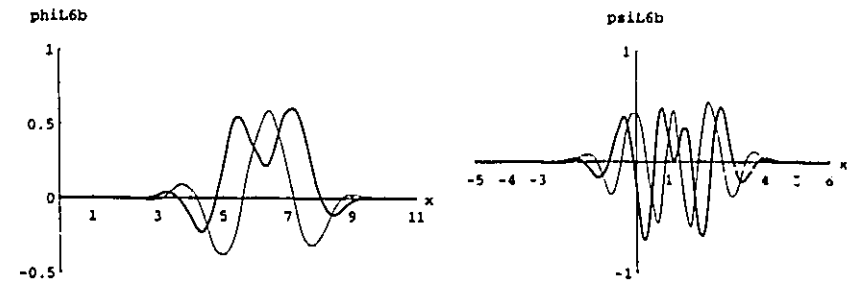


Figure 5.29: Real (bold lines) and imaginary parts of complex scaling function and wavelet L6b with starting value $\delta_{n0}$.

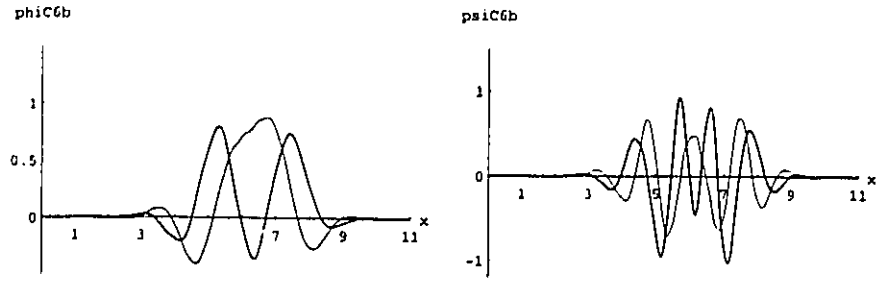


Figure 5.30: Real multiscaling functions and multiwavelets C6b with starting value $[1\ 1]^T\delta_{n0}$.

of the corresponding scaling functions and wavelets as shown in the figures.

We recall that Cooklev's multivawelets, $C_N$, come from Lawton's complex wavelets, $L_N$, in a simple way, but we see from these figures that the shapes of the scaling functions and wavelets of these two kinds dependes upon the starting values used in the cascade algorithm. This can be explained as follows. Since the lowpass filter is of the form

$$H_0(z) = \sum_{k\in\mathbf{Z}} H_k z^{-k},$$

then

$$H_0(1) = \sum_{k\in\mathbf{Z}} H_k.$$

In the case of the G-H-M lowpass filter $H_0(z)$, the eigenvalues of $\frac{1}{2}H_0(1)$ are 1 and $-0.2$. Since $\lambda_1 = 1$ and $|\lambda_2| < 1$, then it follows from Proposition 4.2 that the cascade algorithm will converge to the multiscaling function from any two-vector satisfying Remark 4.2. On the other hand, Cooklev's multifilters coming from Lawton's complex wavelets will satisfy

$$H_0(1) = \frac{1}{2}\sum_{k\in\mathbf{Z}} H_k = I.$$

Hence, all eigenvalues are $\lambda = 1$. Since the Eigenvalue Condition 4.1 is not satisfied, Proposition 4.2 does not apply and the scaling function depends upon the starting values

$$\begin{bmatrix} a \\ b \end{bmatrix}.$$

For G-H-M and Strang-Strela multiwavelets, the eigenvalue condition implies that there exists no matrix $M \neq I$ which commutes with the matrix coefficients $H_k$ of the

filter. For Cooklev's multifilters coming from Lawton's complex wavelets, each $H_k$ is of the form

$$H_k = \begin{bmatrix} a_k & -b_k \\ b_k & a_k \end{bmatrix},$$

which represents the complex number

$$z_k = a_k + ib_k.$$

Since matrices of the form $H_k$ commute under matrix product, as does the product of complex numbers, $H_k$ commute with the rotation

$$R = \begin{bmatrix} \cos\alpha & -\sin\alpha \\ \sin\alpha & \cos\alpha \end{bmatrix} \sim \cos\alpha + i\sin\alpha.$$

Thus,

$$R\begin{bmatrix} \phi_1(x) \\ \phi_2(x) \end{bmatrix} = \sqrt{2}\sum_{k\in\mathbf{Z}} RH_kR^TR\begin{bmatrix} \phi_1(2x-k) \\ \phi_2(2x-k) \end{bmatrix} \tag{5.1}$$

$$= \sqrt{2}\sum_{k\in\mathbf{Z}} H_kR\begin{bmatrix} \phi_1(2x-k) \\ \phi_2(2x-k) \end{bmatrix}. \tag{5.2}$$

Hence, $R\Phi$ is produced by the same filter as $\Phi$. In the complex case, this is obvious since

$$e^{i\theta}\phi(x) = \sqrt{2}\sum_{k\in\mathbf{Z}} e^{i\theta}h_ke^{-i\theta}e^{i\theta}\phi(2x-k) \tag{5.3}$$

$$= \sqrt{2}\sum_{k\in\mathbf{Z}} h_ke^{i\theta}\phi(2x-k). \tag{5.4}$$

In Figs. 5.31 and Figs. 5.32 we present "new" multiwavelets whose filter coefficients come from the coresponding multiwavelets filter coefficients, with $N = 3$, multiplied by $e^{i\pi/3}$ and $e^{i\pi/6}$.

It should also be noted that the zeros of the polynomial $Q_A(z)$ in (2.30) of degree $N-1$ for Daubechies' wavelets ${}_Nh_n$ have been obtained by the constructive use of Riesz Lemma in IEEE double-precision floating point arithmetic. Since these zeros are simple, the errors are very small.

To find the zeros of the polynomials ${}_NH(z)$ with $N$ zeros at $z = -1$, quadruple precision was used to obtain the coefficients $h_n$, which are the coefficients ${}_Nh_n$ of

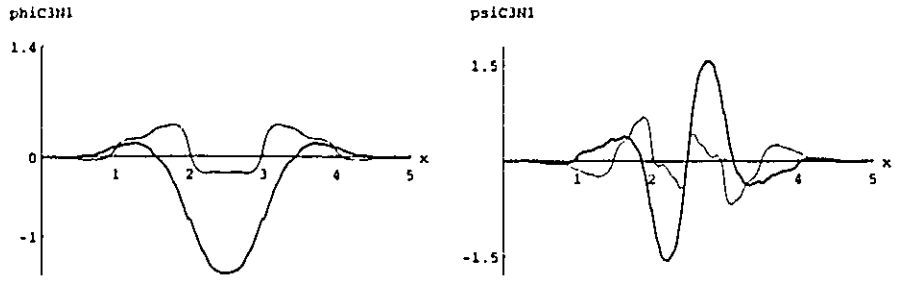


Figure 5.31: New real multiscaling functions and multiwavelets C3N1 with starting value $[\cos(\pi/3) - \sin(\pi/3) \quad \sin(\pi/3) + \cos(\pi/3)]^T$.

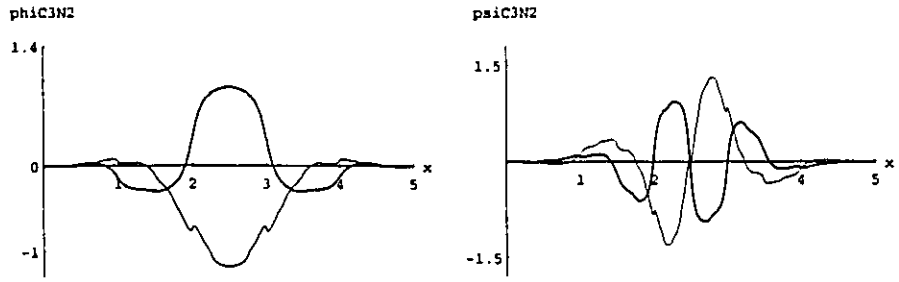


Figure 5.32: New real multiscaling functions and multiwavelets C3N2 with starting value $[\cos(\pi/6) - \sin(\pi/6) \quad \sin(\pi/6) + \cos(\pi/6)]^T$.

Daubechies' filters, of the polynomials $\sum_n h_n z^{-n}$ of degree $2N-1$. The composite root finder of Malek-Vaillancourt [30] and [31] recovers the exact double-precision zeros by means of the $QR$ algorithm in double precision. This root finder is designed to handle polynomials with multiple zeros.

It is to be noted that constructing and evaluating the polynomials in double precision will yield the multiple zeros, $z = -1$, to an error of $10^{-3}$ for $N = 3$. A similar error yields for $N = 4$. This situation gets worse for larger value of $N$.

# Chapter 6

# Conclusion

The object of this thesis was to study and compare different kinds of one-dimensional wavelets with emphsisis on complex-valued scalar wavelets and real-valued multi-wavelets.

The usual approximating method used in the plotting of wavelets, which is called "cascade algorithm", was described. Several sets of real-valued scalar wavelets, complex-valued scalar wavelets and multiwavelets with the same vanishing moments and the corresponding scaling functions were obtained by this algorithm.

Complex-valued scalar wavelets are the extension of Daubechies' real-valued scalar wavelets, and they offer possibilities to achieve properties,such as symmetry, which cannot be achieved in the real case .

We studied the construction and the properties of the complex-valued wavelets. It is quite remarkable that the imaginary part of the scaling function is an admissible wavelet since its integral vanishes. Since the complex filter coefficients may produce some redundancy, and people did not pay much attention to it, the study and use of complex-valued wavelets is more recent. Recent studies in physics show that the symmetry property permits the use of symmetrization in signal analysis to avoid border effects. Therefore, some physicists and engineers began to pay more attention to the development of the wavelet theory. Recent contributions are due to J.-M. Lina *et al.* They generalized the solution of the orthogonality conditions for complex-valued wavelets and constructed the symmetric multiresolution analysis on $[0, 1]$. The associated quadrature mirror filter (QMF) which exhibits the underlying symmetry of the analyzing function should be of interest in image analysis.

Multiwavelets is a very recent topic. Many properties of multiwavelets should be considered with matrix theory since the coefficients of filters are matrices and the theory of scalar wavelets cannot be generalized in a straighforward way. The theory for multiwavelets is still in the development and experimental stage. The general idea was reviewed and several examples were studies in the thesis. The general expression for the determinant of the product filter $P(z)$, which appears in the general design method, have not been completely studied, and this research will remain active in the future.

Some comparisons between Daubechies' wavelets, Lawton's wavelets and multiwavelets are made, but it will be worth making a more detailed comparison. Since there are still many unclear differences among them, it may be useful to understand the factors which cause these diffences for the implementation of the wavelet theory.

Although the wavelet theory and its applications have been extensively studied and received quick development, there are still many challenging questions without answers.

# Bibliography


[1] R. Ashino, M. Nagase, and R. Vaillancourt, *On a construction of multiwavelets*, Comp. Math. Applic., to appear.

[2] A. Cohen, *Ondelettes, analyses multirésolutions et filtres miroirs en quadrature*, Ann. Inst. H. Poincaré, **7**, (1990), 439–459.

[3] A. Cohen, I. Daubechies, and J.-C. Feauveau, *Biorthogonal bases of compactly supported wavelets*, Comm. Pure Appl. Math., **45**, no. 5, (1992), 485–560.

[4] A. Cohen, I. Daubechies, and G. Plonka, *Regularity of refinable function vectors*, preprint, Rostock University, (1996).

[5] T. Cooklev, *Regular perfect-reconstruction filter bank and wavelet bases*, Ph.D. Thesis, Tokyo Institute of Technology, 1995.

[6] T. Cooklev, M. Kato, A. Nishihara, and M. Sablatash, *Multifilter banks and multiwavelet bases*, IEIGE Tech. Rept. IE95-22, May 1995.

[7] T. Cooklev, A. Nishihara, M. Kato, and M. Sablatash, *Two-channel multifilter banks and multiwavelets*, preprint.

[8] T. Cooklev, A. Nishihara, T. Yoshida, and M. Sablatash, *Multidimensional linear phase FIR digital filter banks and wavelet base*, Proc. 9th Digital Signal Process, Workshop, Kyoto, Japan, 1994, pp. 463–468.

[9] T. Cooklev, A. Nishihara, T. Yoshida, and M. Sablatash, *New multidimensional nonseparable linear phase wavelet filters*, preprint.

[10] I. Daubechies, *Orthonormal bases of compactly supported wavelets*, Comm. Pure Appl. Math., **41**, no. 7, (1988), 909–996.

[11] I. Daubechies, *Ten lectures on wavelets*, Society for Industrial and Applied Mathematics, Philadelphia PA, 1992.

[12] I. Daubechies and J. C. Lagarias, *Two scale difference equations II, Local regularity, infinite products of matrices and fractals*, SIAM. J. Math. Anal., **23**, no. 4, (1992), 1031–1079.

[13] G. Deslauriers and S. Dubuc, *Interpolation dyadique*, Fractals, dimensions non entières et applications, Masson, Paris, 1987, pp. 44–55.

[14] G. Donavan, J. Geronimo, D. Hardin and P. R. Massopust, *Construction of orthogonal wavelet using fractal interpolation functions*, SIAM J. Math. Anal. **, (1996), ***–***.

[15] J. Geronimo, D. Hardin, and P. R. Massopust, *Fractal functions and wavelet expansions based on several scaling functions*, J. Approx. Theory, **78**, (1994), 373–401.

[16] A. Grossman and J. Morlet, *Decomposition of Hardy functions into square integrable wavelets of constant shape*, SIAM J. Math. Anal., **15**, (1984), 723–736.

[17] A. Haar, *Zur Theorie der orthogonalen Funktionensysteme*, Math. Ann. **69**, (1910), 331–371.

[18] C. Heil and D. Colella, *Matrix refinement equations: Existence and uniqueness*, preprint, (1994).

[19] J.-P. Kahane, Y. Katznelson and K. de Leeuw, *Sur les coefficients de Fourier des fonctions continues*, C. R. Acad. Sci. Paris Ser. A-B, **285**, (1977), A1001–A1003.

[20] A. Karoui, *Multidimensional wavelets and applications*, Ph.D. Thesis, University of Ottawa, 1995.

[21] A. Karoui and R. Vaillancourt, *Families of biorthogonal wavelets*, Comp. Math. Applic., **28**, no. 4, (1994), 25–39.

[22] W. Lawton, *Applications of complex valued wavelet transforms to subband decomposition*, IEEE Trans. Signal Processing, **41**, no. 12, (Dec. 1993), 3566–3568.

[23] W. Lawton, *Tight frames of compactly supported wavelets*, J. Math. Phys., **31**, (1990), 1898–1901.

[24] W. Lawton, *Necessary and sufficient conditions for constructing orthonormal wavelet bases*, J. Math. Phys., **32**, (1991), 57–61.

[25] J.-M. Lina and L. Gagnon, *Image enhancement with symmetric Daubechies wavelets*, SPIE, Vol. 2569, San Diego 1995.

[26] J.-M. Lina and M. Mayrand, *Complex Daubechies wavelets*, Appl. and Comput. Harmonic Anal., **2**, (1995), 219–229.

[27] J.-M. Lina and M. Mayrand, *Parametrizations for Daubechies wavelets*, Phys. Rev., **E48**, (Dec. 1993).

[28] J.-M. Lina, *Image processing with complex Daubechies wavelets*, PHYSNUM, Centre de recherches mathématiques, Université de Montréal, Montréal, Québec, Canada H3C 3J7, Sept. 1995.

[29] S. Mallat, *Multiresolution approximations and wavelet orthonormal bases of* $L^2(\mathbb{R})$, Trans. Amer. Math. Soc., **315**, (1989), 69–88.

[30] F. Malek and R. Vaillancourt, *Polynomial zerofinding iterative matrix algorithms*, Computers Math. Applic. Vol. 29, no. 1, (1995), 1–13.

[31] F. Malek and R. Vaillancourt, *A composite polynomial zerofing matrix algorithm*, Computers Math. Applic., Vol. 30, no. 2, (1995), 37–47.

[32] Y. Meyer, *Wavelets and operators*, transl. from the French by D. H. Salinger, Cambridge Studies in Advanced Mathematics, **37**, Cambridge University Press, Cambridge, UK, 1992.

[33] G. Plonka and V. Strela, *Construction of multi-scaling functions with approximation and symmetry*, preprint, Rostock University, (1996).

[34] Z. Shen, *Refinable function vectors*, preprint, National University of Singapore, 1996.

[35] G. Strang and T. Nguyen, *Wavelets and filter banks*, Wellesley-Cambridge Press, Box 812060, Wellesley MA 02181, 1996.

[36] G. Strang and V. Strela, *Short wavelets and matrix dilation equations*, IEEE Trans. on Signal Processing, **43**, (1995), 108–115.

[37] G. Strang and V. Strela, *Orthogonal multiwavelets with vanishing moments*, J. Optical Eng, **33**, (1994), 2104–2107.

[38] V. Strela, *Multiwavelets: Regularity, orthogonality and symmetry via two-scale similarity transform*, preprint, Dep. Math., MIT, Cambridge MA 02139, USA, strela@math.mit.edu.

[39] V. Strela, P. N. Heller, G. Strang, P. Topiwala, and C. Heil, *The application of multiwavelet filterbanks to signal and image processing*, preprint.

[40] P. P. Vaidyanathan, *Multirate systems and filter banks*, Prentice-Hall, Englewood Cliffs, NJ, 1993.

[41] M. Vetterli, *Filters banks allowing perfect reconstruction*, Signal Processing, **10**, no. 3, (1986), 219–244.

[42] M. Vetterli and C. Herley, *Wavelets and filter banks: Theory and design*, IEEE Trans. Signal Proc., **40**, no. 9, (1992), 2207–2232.

[43] D. C. Youla and N. N. Kuzanjian, *Bauer-type factorization of positive matrices and the theory of matrix polynomials orthogonal on the unit circle*, IEEE Trans. Circuits Syst., **25**, no. 2, (Feb. 1978), 57–69.